The origin of nitrogen in Earth's mantle: constraints from basalts 15 N/ 14 N and N2/ 3 He ratios

Jabrane Labidi

The origin of nitrogen in Earth's mantle: constraints from basalts $^{15}N/^{14}N$ and $N_2/^3He$ ratios

J. Labidi[1]

[1] Université de Paris, Institut de physique du globe de Paris, CNRS, Paris, France

Abstract

Plate tectonics is thought to be a major driver of volatile redistribution on Earth. The budget of nitrogen in Earth's mantle has been suggested to be almost entirely surface-derived. Recycling would contribute nitrogen with relatively heavy $^{15}N/^{14}N$ isotope ratios to Earth's mantle. This could explain why the Earth's mantle $^{15}N/^{14}N$ isotope ratio is substantially higher than both solar gases and chondritic parent bodies akin to enstatite chondrites. Here, published nitrogen isotope data of mid-ocean ridge and ocean island basalts are compiled and used to evaluate the nitrogen subduction hypothesis. Nitrogen isotope ratios are used in conjunction with published $N_2/^3He$ and K_2O/TiO_2 ratios on the same basalts. Assuming that ^3He is not recycled, $N_2/^3He$ ratios are argued to trace nitrogen addition to mantle sources via subduction. Various mantle source enrichments for basalts are tracked with K_2O/TiO_2 ratios: elevated K_2O/TiO_2 ratios are assumed to primarily reflect the contributions of recycled components in the basalts mantle sources. The main result of our data compilation is that for most basalts, $\delta^{15}N$ and $N_2/^3He$ remain constant across a vast range of K_2O/TiO_2 ratios. Mid-ocean ridge basalts have $\delta^{15}N$ signatures that are lower than air by ~ 4‰ and an average $N_2/^3He$ ratio of 3.7 (±1.2) $x10^6$ (95% confidence, n= 30). Published $\delta^{15}N$ and $N_2/^3He$ are invariant across K_2O/TiO_2 ratios that vary over a factor of ~ 20. Using estimates of slab K_2O/TiO_2 and $[TiO_2]$, the observed invariant $\delta^{15}N$ and $N_2/^3He$ may

be fit with slabs containing ~0.1 ppm N. A mass balance shows that adding ~10% recycled slabs to the convective mantle only raises the $N_2/^3He$ by < 5%. Lavas from Iceland, Galapagos and Hawaii have high $^3He/^4He$ and $^{15}N/^{14}N$ ratios relative to the convective mantle. Only seven samples show nitrogen isotopic signatures that are unaffected by air contamination, although those samples are poorly characterized for $N_2/^3He$. The seven basalts show $\delta^{15}N$ between –2 and 0‰ that do not vary systematically with K_2O/TiO_2 ratios that vary over a factor of ~ 5. The $N_2/^3He$ ratios of these seven basalts is unknown, but the high $^3He/^4He$ mantle may be estimated by combining published $N_2/^{36}Ar$ to $^3He/^{36}Ar$ ratios. This yields a $N_2/^3He$ of 2.3 (±1.2) x 10^6 (1σ uncertainty). This is indistinguishable from the MORB estimate of 3.7 (±1.2) x 10^6. Invariant $\delta^{15}N$ across variable degrees of mantle enrichments and MORB-like $N_2/^3He$ for the high $^3He/^4He$ mantle are not consistent with nitrogen addition to plume sources with elevated $^3He/^4He$ ratios. A $\delta^{15}N$ between –2 and 0‰ for plume sources, only marginally higher than MORB, could be a primordial feature of undegassed mantle reservoirs. Nonetheless, nitrogen subduction may have contributed to a specific array of mantle sources, as revealed by the few published data on basalts with low $^3He/^4He$ ratios. Lavas from the Society plume with low $^3He/^4He$ ratios show an enriched mantle source, and they have elevated $\delta^{15}N \geq +0.5$‰ and $N_2/^3He > 10^7$. For those, the addition of slabs with concentrations of ~ 0.1 ppm N to a mantle source can account for the integrated dataset. To summarize, the published data suggest that nitrogen subduction may explain a sub-set of published N isotope data on basalts, but that N recycling has an overall more limited impact on mantle nitrogen than previously thought.

1. Introduction

Planetary formation and evolution have shaped the budget of volatile elements of Earth's reservoirs. Nitrogen (N) is the main constituent of our atmosphere. Early catastrophic degassing of the mantle, during a magma ocean phase, may have yielded an atmosphere with ~ 1 bar of N_2 partial pressure (Sossi et al., 2020). Modern N subduction may overpower N_2 mantle degassing by a factor of ~ 20 (Busigny et al., 2011), contrasting with earlier suggestions of quantitative overturn of subducted N_2, at least in a warm subduction zone (Fischer et al., 2002; Hilton et al., 2002; Zimmer et al., 2004). Should modern subduction fluxes from Busigny et al., (2011) be applied back in time, they would require that N_2 from the ancient atmosphere was at least partially re-injected in Earth's mantle. This is ground for the concept of nitrogen "ingassing" or "regassing": the N budget of the modern mantle would be accounted for by massive subduction of atmospheric N, erasing any primordial signatures that the distribution of planetary N may have held (Barry and Hilton, 2016; Javoy, 1997).

The $^{15}N/^{14}N$ isotope ratios of various geological reservoirs may illustrate nitrogen regassing. Variations of the $^{15}N/^{14}N$ isotope ratios are quantified with the δ notation, such as $\delta^{15}N = 1000 \times [(^{15}N/^{14}N)/(^{15}N/^{14}N)_{air} - 1]$, and are given in permil. The modern convective mantle is characterized by a $\delta^{15}N$ of ~ – 5‰ (Javoy and Pineau, 1991; Marty and Zimmermann, 1999). It is somewhat comparable to $^{15}N/^{14}N$ observed in other differentiated bodies such as Mars or the Angrite parent body (Abernethy et al., 2013; Grady and Wright, 2003), but distinct from solar and chondritic signatures. Solar wind and comets have $\delta^{15}N$ signatures ~–387±8‰ and +850±150‰ respectively (Füri and Marty, 2015). Chondrites show a more limited, but nonetheless large isotope range. Enstatite Chondrites (EC) have

70 average $\delta^{15}N$ of -20 ± 11‰ (1σ) while CI chondrites have $\delta^{15}N$ of 48 ± 9‰ (1σ) (Alexander et
71 al., 2012; Grady and Wright, 2003; Pearson et al., 2006). The negative $\delta^{15}N$ observed in bulk
72 EC is consistent with an enstatite chondrite model for Earth's origin (Javoy, 1998, 1997,
73 1995). Interestingly, enstatite chondrites are *even more* depleted in ^{15}N than Earth's mantle
74 at the 1σ level. Should the EC parent body be a major contributor of Earth's nitrogen, a
75 mechanism might have to be invoked to explain the raised $\delta^{15}N$ for Earth's mantle. Mantle N
76 could result from mixing between various types of chondrites including a substantial EC
77 contribution (Javoy, 1997; Marty and Zimmermann, 1999; Piani et al., 2020). Alternatively,
78 terrestrial N could have been delivered by EC parent bodies exclusively. In this scenario, the
79 $\delta^{15}N$ of bulk Earth is ~ -20‰ and planetary differentiation is required to fractionate
80 nitrogen isotopes to account for a mantle $\delta^{15}N$ of ~ -5‰. Core/mantle N isotope
81 fractionations could account for the observations, although the exact value of the
82 metal/silicate $^{15}N/^{14}N$ fractionation factor remains debated (Dalou et al., 2019; Li et al.,
83 2016).

84 One complication for attempts at constraining the nitrogen origin on Earth is the
85 composition of air. Modern air is made of 78% N_2. In terms of absolute quantity, air could
86 host about as much nitrogen as the entire Earth's mantle (Marty, 2102). Air has a $\delta^{15}N$ of
87 0‰, heavier than the modern mantle by $\sim$ 5‰. This heterogeneity reflects a nitrogen
88 isotope disequilibrium between Earth's mantle and surface (Boyd and Pillinger, 1994;
89 Cartigny and Marty, 2013). A mixture of chondritic parent bodies, and/or the expression of
90 metal/silicate fractionations, alone, may not explain the isotope imbalance between the
91 mantle and air. A possible explanation to all the data involves plate tectonics, rather than
92 planetary differentiation. In mantle-surface exchange scenarios, the $\delta^{15}N$ value of –5‰ of

Earth's mantle results from the addition of surface nitrogen with $\delta^{15}N > 0‰$ into a mantle with a starting $\delta^{15}N \leq -20‰$ (Cartigny et al., 1997; Javoy, 1998; Javoy et al., 1986, 1984; Palot et al., 2012). In this hypothesis, the bulk of the Earth would be composed of material similar to enstatite chondrites, but a large proportion of the nitrogen now present in the atmosphere and crust was added by carbonaceous chondrites and/or comets (Halliday, 2013; Javoy, 1997; Marty et al., 2016). The two reservoirs would exchange via subduction, eventually leading to the present isotope imbalance. The $\delta^{15}N$ disequilibrium between air and the mantle would reflect a snapshot of two reservoirs that have not reached complete homogenization yet.

The subduction hypothesis has the merit to offer explanations to both the mantle $\delta^{15}N$ and the isotope imbalance. It is consistent with hypotheses based on modern N fluxes (Busigny et al., 2011; Goldblatt et al., 2009) and indirectly supported by experimental studies showing that recycled nitrogen may be stable as NH_4^+ in potassium-bearing minerals at high pressure and temperature (Watenphul et al., 2010, 2009). However, the subduction hypothesis has requirements that do not seem to be met by observations. By nature, exchange models require a secular decrease in atmospheric N_2 partial pressure and $\delta^{15}N$, and an increase in the mantle N concentration and $\delta^{15}N$ with geological time. It was suggested that surface nitrogen must have had $\delta^{15}N > 20‰$ in the Archean, so that it can balance a negative $\delta^{15}N$ for an enstatite-like Earth's mantle (Javoy, 1997). Similarly, a N_2 partial pressure in the Archean could have been higher than present-day by a factor of 2 (Busigny et al., 2011; Goldblatt et al., 2009). However, available geological evidence do not substantiate the notions of high $\delta^{15}N$ or high N_2 partial pressures at the Earth's surface in the Precambrian (Ader et al., 2016; Marty et al., 2013; Pinti et al., 2001). If anything, both $\delta^{15}N$ of

Archean rocks and N_2 partial pressures in Archean air might have been *lower* than in present-day (Avice et al., 2018; Marty et al., 2013; Pinti et al., 2001; Stüeken et al., 2021), at odds with the requirements of the subduction hypothesis.

The goal of this study is to discuss the merits and the limitations of the subduction hypothesis, but mostly from the point of view of N isotope signatures of mid-ocean ridge basalts (MORB) and ocean island basalts (OIB). Compiled data from the literature are used to show that basalts tapping both the convective mantle and high $^3He/^4He$ plumes have invariant $\delta^{15}N$ across a vast range of mantle enrichment. A mass balance suggests that subducted slabs have N concentrations lower than the rest of the mantle by a factor of 3 or more. Published N isotope data are inconsistent with subducted nitrogen overwhelming the convective mantle, which relaxes the need for substantial exchange between the Earth's surface and mantle over geological times. Alternative set of circumstances to explain the N isotope imbalance are discussed.

2. Basalt geochemistry

Basalts erupted in various geodynamical settings sample multiple mantle reservoirs. Mid-ocean ridge basalts (MORB) sample the convective mantle over ~45,000 kilometers of active ridges. Ocean island basalts (OIB) tap deeper mantle sources, with extreme geochemical signatures associated with mixtures of primordial and recycled components (Kurz et al., 1982; Zindler and Hart, 1986). Upon eruption on the seafloor, basalts are quenched. Glassy rims preserve magmatic vesicles enriched in volatiles, essential to constrain the gas budget of mantle reservoirs. The noble gas systematics for MORB and OIB bring powerful constraints on the origin of Earth's volatile and on the mantle–atmosphere

systems, as presented in various review articles (Graham, 2002; Moreira, 2013; Mukhopadhyay and Parai, 2019). Briefly, MORB have average $^{3}He/^{4}He$ of 8±1 R_A, where R_A is air $^{3}He/^{4}He$. OIB show much larger variations, with $^{3}He/^{4}He$ typically between ~ 5 and >20 R_A. Basalts from Iceland, Loihi and Galapagos have $^{3}He/^{4}He$ typically > 30 R_A (Füri et al., 2010; Hilton et al., 1999; Kurz et al., 2009, 1982). Elevated $^{3}He/^{4}He$ ratios likely represent melts of relatively undegassed regions of the mantle, with low time-integrated (Th-U)/He ratios, compared to MORB (Kurz et al., 1982). The convective mantle likely underwent catastrophic degassing early in Earth's history, followed by slow continuous degassing that continues to the present day (Allègre et al., 1987; Moreira et al., 1998; Sarda et al., 1988).

On average, about ~10% of the convective mantle is made of recycled oceanic crust (Sobolev et al., 2007). This notion is coined the "marble-cake mantle" (Allègre and Turcotte, 1986). The recycled crust essentially acts as means to replenish the mantle with surface-derived components, which is helpful in models relying on volatile subduction: recycled crust is a likely candidate as the carrier of surface-derived volatile in basalt sources. The elemental ratio K_2O/TiO_2 is an easy–to–measure proxy of recycled components in a mantle source. Low $K_2O/TiO_2 < 0.09$ are characteristics of depleted mantle sources (Langmuir et al., 1992; Reynolds et al., 1992; Shen and Forsyth, 1995), hosting limited amounts of recycled components. Higher K_2O/TiO_2 ratios reflect larger contributions of subducted components in mantle sources (Jackson and Dasgupta, 2008). They are typically associated with high La/Sm (Schilling et al., 1983), radiogenic $^{87}Sr/^{86}Sr$ ratios (Jackson and Dasgupta, 2008), and a diverse range of incompatible elements signatures (Bach et al., 1994; Dosso et al., 1999; Le Roex et al., 1989; Le Roux et al., 2002; Schilling et al., 1983). The range in trace element signatures illustrate the compositional variability of enriched mantle sources (Willbold and

Stracke, 2006). At order-zero however, K_2O/TiO_2 ratios act as a generic tracer of subducted components in a mantle source (Jackson and Dasgupta, 2008; Michael and Cornell, 1998; Workman and Hart, 2005).

Nitrogen recycling in a basalt source may be quantified using $\delta^{15}N$, $N_2/^{36}Ar$ and $N_2/^{3}He$ ratios of a glass. If mantle nitrogen is of recycled origin, trends can be predicted between $\delta^{15}N$ and K_2O/TiO_2 ratios, as a function of various nitrogen concentrations in recycled slabs. Because mantle ^{3}He is not recycled in origin (Porcelli et al., 2002), $N_2/^{3}He$ ratios are also anticipated to increase across addition of nitrogen in enriched MORB sources. However, air contamination during eruption or sample handling is the main impediment on determining mantle $\delta^{15}N$, $N_2/^{36}Ar$ and $N_2/^{3}He$ ratios. A measurement strategy has been to crush basalts under ultra-high vacuum and determine simultaneously $\delta^{15}N$, $^{40}Ar/^{36}Ar$, $N_2/^{36}Ar$ and sometimes $^{3}He/^{4}He$ and $N_2/^{3}He$ ratios (Marty, 1995; Marty and Humbert, 1997; Marty and Zimmermann, 1999). Data would be plotted in spaces featuring an isotope or elemental noble gas ratio of interest versus an unambiguous tracer of air contamination. So far, $\delta^{15}N$ and $N_2/^{36}Ar$ would be plotted against the measured argon isotope ratio $^{40}Ar/^{36}Ar$, so mantle $\delta^{15}N$ and $N_2/^{36}Ar$ could be determined by extrapolation (Marty, 1995; Marty and Humbert, 1997; Marty and Zimmermann, 1999). In the following, I summarize the results obtained in previous work with respect to $\delta^{15}N$ mantle estimates from basalts that underwent variable degrees of air contamination. I subsequently address whether the nitrogen systematics in MORB and OIB show any consistency with K_2O/TiO_2.

3. MORB data

A nitrogen isotope dataset including a total of 50 MORB is available in supplementary table 1. The data source is Marty and Humbert (1997), Marty and Zimmermann (1999) and Barry and Hilton (2016). Nitrogen isotope data for three popping rocks are also used, from Javoy and Pineau (1991) and Labidi et al., (2020). The latter study was selected as nitrogen isotope ratios were measured together with Δ_{30} values, an independent measure of air contamination for nitrogen in natural samples (Labidi and Young, 2022).

On Fig. 1, MORB K_2O/TiO_2 data are shown against the magnesium oxide MgO as a tracer of magmatic differentiation. Small symbols are for global MORB, compiled using the PetDB database (www.earthchem.org/petdb, Lehnert et al., 2000). Larger symbols reflect the set of basalts discussed in this study, for which $\delta^{15}N$ data are available in the literature (supplementary table 1). Most MORB show K_2O/TiO_2 ratios varying between 0.02 and 0.40, independent of the degree of basalt differentiation (Fig. 1). The low end of the K_2O/TiO_2 range is associated with a depleted mantle reservoir, while the high end of the range reflects contributions from enriched slabs. Recycled components have K_2O/TiO_2 ratios ~ 0.5, inherited from the composition of the igneous oceanic crust (Kelley et al., 2003) and/or various types of recycled sediments (Plank and Langmuir, 1998).

3.1. The $^{15}N/^{14}N$ ratio

Basalts from mid-ocean ridges tend to show negative $\delta^{15}N$ (Cartigny et al., 2001; Javoy and Pineau, 1991; Marty and Humbert, 1997; Marty and Zimmermann, 1999). Basalts with air-like $^{40}Ar/^{36}Ar$ show a ~10‰ range in $\delta^{15}N$ (Fig. 2). This may reflect the assimilation of hydrothermal nitrogen after it experienced $\delta^{15}N$ fractionation (Marty and Zimmermann,

1999). This is consistent with the observation of $^{36}Ar/^{22}Ne$ ratio of hydrothermal waters for basalts with air-like $^{40}Ar/^{36}Ar$ ratios (Peron et al., 2019). At elevated mantle-like $^{40}Ar/^{36}Ar$ ratios, basalts show a consistent depletion for $^{15}N/^{14}N$ akin to the signatures observed in peridotitic diamonds (Cartigny et al., 2014), with a $\delta^{15}N \sim -4‰$. This is interpreted as the signature of the convective mantle tapped by mid-ocean ridge basalts (Marty and Zimmerman, 1999).

3.2. the $N_2/^{36}Ar$ ratio

The $N_2/^{36}Ar$ global basalt dataset is shown in Fig. 3. Data are from the same references as Fig. 2. At atmospheric $^{40}Ar/^{36}Ar$ ratios of ~300, $N_2/^{36}Ar$ is also atmospheric, i.e., 2.5×10^4. At mantle-like $^{40}Ar/^{36}Ar$ values of > 10,000, $N_2/^{36}Ar$ ratios are higher, up to 4×10^6. The available data are too scattered to allow identifying a trend. A global $N_2/^{36}Ar$ – $^{40}Ar/^{36}Ar$ correlation is apparent only when logarithm scales are used for the plot (Fig. 3B). Despite the scatter and the few outliers, the trend indicates at first order that the N_2 and Ar overprints by air-derived components are concomitant, masking elevated $N_2/^{36}Ar$ ratio of the MORB source.

Taking the $N_2/^{36}Ar$ – $^{40}Ar/^{36}Ar$ correlation has global significance, and assuming the $^{40}Ar/^{36}Ar$ of the convective mantle is ~25,000±2,000 (Moreira et al., 1998; Mukhopadhyay, 2012; Péron et al., 2019), a $N_2/^{36}Ar$ ratio of $2.0^{+1.0}_{-1.2} \times 10^6$ is obtained for the convective mantle. This ratio is robust, since nitrogen and argon are not fractionated during basalt degassing, on account of a similar solubility with respect to CO_2-rich magmatic vesicles (Libourel et al., 2003; Marty, 1995). One potential issue however is that the trend on Fig. 3B is driven by extractions on one basalt from the mid-Atlantic ridge, CH98 DR11, which yielded

some of the highest $^{40}Ar/^{36}Ar$ ratios ever reported for MORB of 42,335 ± 9713 (Marty and Humbert, 1997). Whether this basalt may represent an appropriate endmember to drive the $N_2/^{36}Ar$ – $^{40}Ar/^{36}Ar$ relation and thus characterize the entire convective mantle is unclear.

3.3. The $N_2/^3He$ ratio

The $N_2/^3He$ data are shown against the argon isotope ratio $^{40}Ar/^{36}Ar$ in Fig. 4. Data are the MORB in Marty and Zimmerman (1999), as well as the so-called "popping" rock by Javoy and Pineau (1991). In this space, mixings are not on straight lines. The curvature of mixing relationships is defined by the $[^3He/^{36}Ar]_{air}/[^3He/^{36}Ar]_{mantle}$ ratio. The $^3He/^{36}Ar$ air value is 2.5×10^{-7}, considerably lower than the upper-mantle value of $\sim 5.0 \times 10^{-1}$ (Moreira et al., 1998; Péron et al., 2019; Raquin et al., 2008), thus the $[^3He/^{36}Ar]_{air}/[^3He/^{36}Ar]_{mantle}$ ratio is different from unity by 6 orders of magnitude. This results in air–mantle mixings on extremely curved hyperbolae (Fig. 4). As a result, any basalt with a $^{40}Ar/^{36}Ar > 500$ plots on the near-horizontal branch of the $N_2/^3He$ – $^{40}Ar/^{36}Ar$ mixing hyperbola (Fig. 4). In other words, a basalt with a $^{40}Ar/^{36}Ar > 500$ shows a $N_2/^3He$ ratio broadly similar to the uncontaminated basalt endmember. The popping rock 2πD43 yields a $N_2/^3He$ of 3.0±0.1 x 10^6 (5 orders of magnitude below the air value of $\sim 10^{11}$) at $^{40}Ar/^{36}Ar$ ratios ~5,000 (Javoy and Pineau, 1991), which is considered a sound representation of its mantle source. A similar estimate was recently obtained in Marty et al., (2020), but with no $^{40}Ar/^{36}Ar$ measurement.

MORB analyzed by Marty and Zimmerman (1999) have an average $N_2/^3He$ of 1.4±0.6 x 10^6 (95% confidence, n=30) which at face value appears lower than the popping rock value by a factor of ~ 2 (Fig. 4A). Helium is 2 to 10 times more soluble than N_2 in basaltic melts

(Libourel et al., 2003 and references therin). Magmatic degassing often occurs under a Rayleigh distillation, where vesicles are continuously nucleated and immediately lost from melts (Cartigny et al., 2001; Marty and Zimmermann, 1999). Thus, measured elemental ratios of ordinary MORB can be considerably different from the starting compositions, leading to confusion with regard to the true N_2/He ratio of a parental melt. To reconstruct the starting $N_2/^3He$ value, the $^4He/^{40}Ar^*$ tracer is particularly useful ($^{40}Ar^*$ only takes into account the fraction of ^{40}Ar that is not air-derived, Staudacher et al., 1989). Helium is fractionated from argon by degassing solubility rules. The starting $^4He/^{40}Ar^*$ is set at ~1.5, as observed in popping rocks and constrained by the U/K ratio of the mantle (Moreira et al., 1998). In the MORB from Marty and Zimmermann (1999), $^4He/^{40}Ar^*$ vary over more than one order of magnitude, suggesting volatile ratio reflect considerable fractionation. Following Marty and Zimmermann (1999), reconstructed $N_2/^3He$ ratios are on average 3.7 (±1.2) x 10^6 (n=30, 95% conf), indistinguishable from the popping rock value of 3.0 (±0.1) x 10^6 (Fig. 4B). In this work, I adopt this ratio as the estimate of the convective mantle.

4. **Ocean island basalts**

A nitrogen isotope dataset including a total of 44 OIB is available in supplementary table 2. The data source is Marty and Humbert (1997), Sano et al., (2001), Marty and Dauphas (2003), and Halldorson et al., (2016). Note that only 5 out of the 42 basalts characterized in Halldorson et al., (2016) were used in the data compilation. The five basalts were selected on the basis of their $^{40}Ar/^{36}Ar > 500$. The other 37 samples with $^{40}Ar/^{36}Ar < 500$ from Halldorson et al., (2016) are nonetheless plotted on Fig. 2.

The OIB dataset is broken down in two groups: lavas with $^{3}He/^{4}He \leq 7.5\ R_A$ and with $^{3}He/^{4}He \geq 8\ R_A$. A total of 26 lavas from Society with $^{3}He/^{4}He \leq 7.5\ R_A$ were investigated for $\delta^{15}N$, $N_2/^{36}Ar$ and $^{40}Ar/^{36}Ar$ (Marty and Dauphas, 2003). Out of those, 13 have $^{40}Ar/^{36}Ar >$ 500, including only 5 with measured $N_2/^{3}He$ ratios. On the other side of the spectrum, 18 OIB with $^{3}He/^{4}He \geq 8\ R_A$ from Iceland, Hawaii and Galapagos were investigated for $\delta^{15}N$, $N_2/^{36}Ar$ and $^{40}Ar/^{36}Ar$. Out of those, 12 basalts have $^{40}Ar/^{36}Ar \geq 500$ and simultaneous measurements of $\delta^{15}N$, $N_2/^{36}Ar$, $^{40}Ar/^{36}Ar$, including 8 samples with measured $N_2/^{3}He$ ratios.

4.1 $^{15}N/^{14}N$ ratios

Nitrogen isotope measurements were made on volatile fractions showing $^{40}Ar/^{36}Ar$ of up to ~3,300 for Iceland, (Marty and Dauphas, 2003), 2635±5 for Galapagos (Marty and Humbert, 1997) and ~ 700 for Loihi (Sano et al., 2001). The Galapagos, Hawaii and Iceland mantle sources are characterized by $^{40}Ar/^{36}Ar$ of ~10,000±2,000 (Mukhopadhyay, 2012; Péron et al., 2016; Trieloff et al., 2000), so $\delta^{15}N$ values have to be taken with caution. At the highest $^{40}Ar/^{36}Ar$, $\delta^{15}N$ range between +0.6‰ and –1.9‰ (Fig. 2). For Society, data from Marty and Dauphas (2003) show $^{40}Ar/^{36}Ar$ up to 9995±550. At the highest $^{40}Ar/^{36}Ar$, $\delta^{15}N$ are observed between +0.4 and~+3.6‰ (Fig. 2B).

4.2 The $N_2/^{36}Ar$ ratio

If extrapolating the data for basalts with high $^{3}He/^{4}He$ at a $^{40}Ar/^{36}Ar$ of ~10,000, the $N_2/^{36}Ar$ backed out from the trend on Fig. 3 is $0.7^{+0.5}_{-0.3} \times 10^{6}$. Although not statistically different from the convective mantle, this estimate allows somewhat lower $N_2/^{36}Ar$ for the plume mantle, as suggested originally by Dauphas and Marty (1999). Under the assumption

299 of a unique ln[$^{40}Ar/^{36}Ar$]–ln[$N_2/^{36}Ar$] trend and $^{40}Ar/^{36}Ar > 10{,}000$, data on Society basalts
300 would yield a somewhat higher $N_2/^{36}Ar$ than Iceland (Fig. 3B).
301
302 **4.3 The $N_2/^3He$ ratio**
303 The dataset on Galapagos and Iceland basalts, from Marty and Dauphas, (2003), does
304 not allow compiling $N_2/^3He$ ratios (supplementary Table 2). For Iceland basalts, Marty et al.,
305 (2020) published a $N_2/^3He$ estimate of ~ 3 x 10^6 for a DICE glass. The data is presented
306 without a $^{40}Ar/^{36}Ar$ measurement and therefore cannot be plotted on Fig. 4, but it is
307 consistent with a MORB-like $N_2/^3He$ for the Icelandic mantle source. Other Iceland basalts
308 with $^{40}Ar/^{36}Ar$ between 591 and 1334 from Halldorson et al., (2016) show $N_2/^3He$ of 2.7±3.6
309 x10^6 (95% conf., n=5). After correction from fractional degassing, $N_2/^3He$ averages at
310 3.7±2.9x10^6 (95% conf., n=5). The one Loihi basalt with $^{40}Ar/^{36}Ar$ ~ 700 shows an
311 uncorrected $N_2/^3He$ of 3.1x10^6, which becomes 2.5x10^6 after correction (Sano et al., 2001).
312 Uncorrected $N_2/^3He$ values on basalts from the Society hotspot are up to ~10^9, three
313 orders of magnitude higher than the MORB mantle (Fig. 4A). After correction for fractional
314 degassing following the method of Marty and Zimmermann (1999), the $N_2/^3He$ range to
315 values up to 10^8.
316
317 **5. Discussion**
318 **5.1. MORB data do not support nitrogen regassing**
319 The published dataset for ordinary MORB reveals that $\delta^{15}N$ and $N_2/^3He$ do not vary
320 systematically with K_2O/TiO_2 ratios (Fig. 5 and 6). The 2πD43 popping rock is itself an
321 enriched MORB with a K_2O/TiO_2 estimated at ~0.38 (Sarda and Graham, 1990) or ~0.19

(Cartigny et al., 2008). This sample shows MORB-like $\delta^{15}N$ and $N_2/^3He$ signatures (Javoy and Pineau, 1991, Marty et al., 2020 Fig. 5). Three other popping rocks have $\delta^{15}N$ ~–3‰ associated with near-zero Δ_{30} values, suggesting the extracted N_2 is unaffected by air contamination (Labidi et al., 2020; Labidi and Young, 2022). Those popping rocks have high K_2O/TiO_2 ~ 0.35 (Jones et al., 2019). To account for the data, a mantle component with K_2O/TiO_2 ~0.02 is taken to mix with recycled slabs of indeterminate lithologies but high K_2O/TiO_2 ~0.5. An average K_2O/TiO_2 ~0.5 is an approximation consistent with observations in extreme mantle endmembers (Jackson and Dasgupta, 2008) and in protoliths susceptible to be subducted (Kelley et al., 2003; Plank and Langmuir, 1998).

The flat relationship between $\delta^{15}N$ and K_2O/TiO_2 (Fig. 5) is not simple to reconcile with recycling, if the mantle and slabs have distinct $\delta^{15}N$ signatures as suggested in e.g., Barry and Hilton (2016). One may suggest a mixing hyperbola is at play and all MORB happen to be on the flat portion of the mixing curve in Fig. 5. By design, the curvature of mixing relationships in Fig. 5 is defined by the $[^{14}N/TiO_2]_{slabs}/[^{14}N/TiO_2]_{mantle}$ ratio. Mixing hyperbolae are valid only if N/TiO_2 ratio of the two reservoirs (slabs and mantle) are different, i.e., if slabs have either substantially higher or substantially lower N concentrations relative to the mantle. Below, I explore in detail the viability of the two endmember scenarios.

5.1.1 Scenario 1: slabs have high N concentrations

In a scenario 1, $N/TiO_{2\ slab} > N/TiO_{2\ mantle}$, i.e., slabs have high [N]. This is testing the possibility that the mantle prior to subduction had low [N] and thus low $N_2/^3He$. For this reservoir, I take a $\delta^{15}N$ of ~–20‰, akin the average value of enstatite chondrites. This

scenario embodies the notion of nitrogen regassing: recycling would increase [N], $N_2/^3He$, $\delta^{15}N$ together with K_2O/TiO_2.

I take a $N_2/^3He$ of $3x10^5$ for the mantle prior to slab addition. This ratio is a factor of 10 lower than the observed ratio for the modern MORB mantle. Taking an N concentration of ~0.27±0.16 ppm N for the MORB source (Marty and Dauphas, 2003), a low $N_2/^3He$ by a factor of 10 yields a concentration of ~ 0.03 ppm N for the mantle prior to the addition of slabs. Values even lower would make no difference. I take TiO_2 concentration of 0.13 wt% for the depleted mantle (Workman and Hart, 2005), resulting in a N/TiO_2 of ~2×10^{-5}. For recycled components, I take $N_2/^3He = 10^{11}$ (Sano et al., 2001) and $[TiO_2]$ = 0.4 wt%. The latter is not fundamentally different from $[TiO_2]$ ~ 0.35 and 0.60 wt% for igneous crust and marine sediments, respectively (Kelley et al., 2003; Plank and Langmuir, 1998). Other values for slabs $N_2/^3He$ and TiO_2, within a reasonable range, do not change the main result: when a mixing scenario fits the K_2O/TiO_2 – $\delta^{15}N$ data, recycled nitrogen must have an average $\delta^{15}N$ of –4‰ and slabs must have N concentrations ≥ 10 ppm (Fig. 5A).

This scenario is associated with an array of limitations. Firstly, recycled N with negative $\delta^{15}N$ is inconsistent with published compositions of metasediments and metagabbros with average $\delta^{15}N$ ~ +3‰ (Busigny et al., 2011), even in the Archean (Ader et al., 2016). A $[N]_{slabs}$ ≥ 10 ppm is higher than the N concentrations in fresh MORB of ~1.1 ppm (Marty, 1995). The altered oceanic crust shows [N] up to ~12 ppm, only for the shallowest 1,000 meters of altered basalts (Busigny et al., 2019). Horizons under 1,500 meters under the seafloor show [N] < 2 ppm (Busigny et al., 2019). It is not clear how the recycled oceanic crust could preserve an average [N] as high as 10 ppm *after* subduction.

The most important limitation is that scenario 1 fails to account for the invariant $N_2/^3He$ at varying K_2O/TiO_2 (Fig. 5B). The curvature of mixing relationships in Fig. 5B is defined by the $[^3He/TiO_2]_{slab}/[^3He/TiO_2]_{mantle}$ ratio. Because ^3He is not recycled (Porcelli et al., 2002), the $[^3He/TiO_2]_{slab}/[^3He/TiO_2]_{mantle}$ ratio by necessity is << 1. This always results in hyperbolic mixtures in Fig. 5B, so that homogeneous $N_2/^3He$ at varying K_2O/TiO_2 *cannot* be fit. Slab components with high [N] cause sharp increases in $N_2/^3He$ at varying K_2O/TiO_2, which is not observed. Overall, there is no viable scenario where Earth's convective mantle is overwhelmed by recycled N and at the same time homogeneous $\delta^{15}N$ and $N_2/^3He$ at varying K_2O/TiO_2 ratios are accounted for.

5.1.2 Scenario 2: slabs have low N concentrations

In a scenario 2, I explore the possibility of $N/TiO_{2\ slab} < N/TiO_{2\ mantle}$, i.e., slabs have low [N]. In this scenario, mixing hyperbolae are the inverse of scenario 1, so the starting mantle (prior to the initiation of subduction) inevitably has $\delta^{15}N \sim -4‰$. It is assigned a [N] of 0.3 ppm, a $N_2/^3He$ ratio of $3x10^6$, and a $N/TiO_2 \sim 2x10^{-4}$. Subducted nitrogen is fixed at $\delta^{15}N \sim +3‰$ by observations in metagabbros and metasediments (Bebout et al., 2013; Bebout and Fogel, 1992; Busigny et al., 2019, 2011, 2003; Haendel et al., 1986).

The main result is that N/TiO_2 for slabs must be $\leq 3x10^{-5}$, at least one order of magnitude lower than the mantle, for the mixing curve on Fig. 6 to fit the data. Taking $[TiO_2]$ = 0.4 wt% for recycled components (Kelley et al., 2003; Plank and Langmuir, 1998), it results that $[N]_{slabs} \sim$ 0.1 ppm N. A $[N]_{slabs} \sim$ 0.1 ppm N is not unreasonable: it is lower than N concentrations in the altered oceanic crust, consistent with ≥ 90% nitrogen losses from the slabs – likely occurring underneath sub-arc mantle sources (Füri et al., 2021; Labidi et al.,

2021). The addition of 10 to 20% slabs (with $[TiO_2]_{slabs}$ = 0.4 wt% and K_2O/TiO_2 = 0.5) to a depleted mantle (with $[TiO_2]_{depleted\ mantle}$ = 0.13 wt% and K_2O/TiO_2 = 0.02) returns K_2O/TiO_2 ratios between 0.12 and 0.19, covering most of the enriched-MORB range (Fig. 1). Taking $[N]_{slabs}$ ~0.1 ppm, adding 10 to 20% slabs to a mantle source would cause only a ~3% and ~6% increase of bulk [N] or $N_2/^3He$ respectively, well below the measurement uncertainties.

To summarize, scenario 2 suggests nitrogen subduction is not recorded in most MORB because the concentration of nitrogen in slabs is too low compared to the average mantle. It results that the observed $\delta^{15}N \sim -5‰$ and $N_2/^3He \sim 3x10^6$ may reflect mantle signatures pre-dating the onset of subduction. A summary of this analysis is shown on Fig. 7.

5.2 Nitrogen in plumes

Elevated $\delta^{15}N$ values in plumes may reflect subducted nitrogen with positive $\delta^{15}N$ accumulated in mantle sources (Barry and Hilton, 2016; Bekaert et al., 2021; Dauphas and Marty, 1999; Marty and Dauphas, 2003). Here, published data are separated between basalts sampling (1) low $^3He/^4He$ mantle sources and (2) high $^3He/^4He$ mantle sources.

5.2.1 the case of low $^3He/^4He$ basalts

Basalts from Society do show $\delta^{15}N > 0.5‰$ clearly distinct from MORB (Fig. 2B), with $N_2/^3He$ ratios corrected from fractional degassing being between 10^7 and 10^8 (Fig. 4). However, Society is all but a primordial plume. Lavas show low $^3He/^4He$ ratios, down to ~6 R_A (Marty and Dauphas, 2003), enriched K_2O/TiO_2 ~0.45 (Hemond et al., 1994, Jackson and Dasgupta, 2008), and extreme radiogenic isotope signature (Chauvel et al., 1992). Nitrogen

412 isotopes and K_2O/TiO_2 data were not acquired on the same Society basalts. Given that
413 enriched K_2O/TiO_2 signatures appear homogeneous among basalts from Society (Hémond et
414 al., 1994), a possible Society field may be obtained by combining the N isotope data from
415 Marty and Dauphas (2003) to major element data from Hemond et al., (1994). Nitrogen
416 subduction associated with enriched slabs can account for the resulting field, shown on Fig.
417 5 and 6. Society appears to be a plume with geochemical signatures fully consistent with
418 nitrogen subduction. A similar conclusion was reached for free gases with low $^3He/^4He$ from
419 the Eifel region, Germany : using the new Δ_{30} systematic to account for air contamination,
420 the source of the mantle-derived gases in this particular region was suggested to incorporate
421 subducted nitrogen (Labidi et al., 2020).
422
423 **5.2.2 the case of high $^3He/^4He$ basalts**
424 Lavas from Galapagos, Loihi and Iceland tell a different story than Society. They show
425 $\delta^{15}N$ between –2‰ and 0‰ at their highest $^{40}Ar/^{36}Ar$ ratios (Fig. 2). Those $\delta^{15}N$ values have
426 to be taken with caution, since measurements were done at $^{40}Ar/^{36}Ar$ between ~700 and
427 ~3,300 (supplementary table 2), while the sources of the three plumes have $^{40}Ar/^{36}Ar$ of
428 ~10,000±2,000 (Mukhopadhyay, 2012; Péron et al., 2016; Trieloff et al., 2000). Nonetheless,
429 considering the shape of the mixing curve on Fig. 2, measured $\delta^{15}N$ at $^{40}Ar/^{36}Ar$ > 1,000 are
430 probably not far off the true values for the plume sources.
431 The $N_2/^3He$ ratios for the Galapagos, Loihi and Iceland basalts are not well known
432 (supplementary table 2). Only one Loihi sample with a $^{40}Ar/^{36}Ar$ ratio of ~700 has a
433 published $N_2/^3He$ of $2.5x10^6$ (Sano et al., 2001). For Iceland and Galapagos, a rough $N_2/^3He$
434 reconstruction can be done by combining published $N_2/^{36}Ar$ with $^3He/^{36}Ar$ ratios from the

literature. Taking $N_2/^{36}Ar = 0.7^{+0.5}_{-0.3} \times 10^6$ according to the $N_2/^{36}Ar$ - $^{40}Ar/^{36}Ar$ correlation (Fig. 3), and $^3He/^{36}Ar$ of 0.3 for Iceland (Colin et al., 2015), a $N_2/^3He$ estimate of 2.3 (±1.2) x 10^6 is obtained (1σ uncertainty). If a $^3He/^{36}Ar$ of 0.8 is used (Peron et al., 2016, Mukhopadyay, 2012), a $N_2/^3He$ estimate of 1.6 (±0.9) x 10^6 (1σ uncertainty) would be obtained. These estimates seem indistinguishable from the MORB mantle. This is also consistent with an actual $N_2/^3He$ measurement on a DICE glass performed recently, but with no $^{40}Ar/^{36}Ar$ data (Marty et al., 2020).

Halldorson et al. (2016) suggested a much higher $N_2/^3He$ ratio of 10^{10} for Iceland, extrapolated from $N_2/^{40}Ar^*$ data. Such a massive N enrichment in Iceland was considered unwarranted (Hirschmann, 2018), as it relies on assuming *all* N_2 to be mantle-derived in basalts with atmospheric $^{40}Ar/^{36}Ar$ ratios. Instead, one may take the measured $N_2/^3He$ (corrected from fractional degassing) of the few basalts with $^{40}Ar/^{36}Ar > 500$ in Halldorson et al., (2016). This results in an average $N_2/^3He$ of 3.7±2.9x10^6 (95% conf., n=5), consistent with the reconstructed $N_2/^3He$ of 2.3 (±1.2) x10^6 and the $N_2/^3He$ estimate of 3.7 (±1.2) x 10^6 for the MORB mantle.

Hydrothermal gases from the Yellowstone stratovolcano yield similar results. Near-zero $\delta^{15}N$ and MORB-like $N_2/^3He$ were shown to be associated with the plume signature using the Δ_{30} approach (Labidi and Young, 2022). A picture of MORB-like $N_2/^3He$ but near-zero $\delta^{15}N$ for the high $^3He/^4He$ mantle seems to emerge as a global feature. It may be tempting to describe the nitrogen budget of the high $^3He/^4He$ mantle as being influenced by recycled slabs, overprinting the potentially primordial $\delta^{15}N$ of solar or enstatite chondrite parent bodies (Barry and Hilton, 2016). Although this is based on a few samples and therefore might change with future work, the $N_2/^3He$ of MORB and of the high $^3He/^4He$

mantle appear indistinguishable, and it is unclear how this may reflect nitrogen recycling in one or in both reservoirs. One possibility involves the true primordial mantle having low $N_2/^3He$ ($< 10^6$). Mixing with a slab showing a high $N_2/^3He$ ($>10^6$) would result in MORB-like $N_2/^3He$ (Bekaert et al., 2021). The $N_2/^3He$ similarity with MORB would be the fortuitous result of mixing between two distinct components in just the right proportions to yield convective mantle values. The basalt data do not support this circumstance. DICE 10 and 11 (Iceland) have low K_2O/TiO_2, of ≤ 0.06 (Brandon et al., 2007), which argues for minimal contributions of recycled components in their mantle source. Both the Loihi glass from Sano et al., (2001) and the Galapagos sample with the highest $^{40}Ar/^{36}Ar$ ratios from Marty and Humbert (1997) have K_2O/TiO_2 of ~0.20 (Geist et al., 2006; Nishio et al., 2007), indicating a higher contribution of enriched components in their mantle sources, yet they all show invariant $\delta^{15}N$ between –2 and 0‰ (supplementary table 2). If confirmed with new data in future work, an invariant $\delta^{15}N$ (and $N_2/^3He$?) at varying K_2O/TiO_2 for OIB probably indicates that like with MORB, recycled components intermingled with the high $^3He/^4He$ mantle may not modify the plume N isotope signatures. A $\delta^{15}N$ between –2‰ and 0‰ for the high $^3He/^4He$ mantle, if truly statistically distinct from MORB, would require an explanation without the need to invoke slab recycling. A summary of this analysis is shown on Fig. 7.

5.3. Revisiting the deep N cycle

The MORB mantle is made of roughly ~10% recycled slabs (Allègre and Turcotte, 1986; Hamelin et al., 2011; Sobolev et al., 2007). The composition of plume basalts with high $^3He/^4He$ also require the occurrence of *some* recycled components in mantle sources (Farley

et al., 1992; Hilton et al., 1999; Jackson et al., 2020). Yet, outside of extreme mantle enrichment such as seen in Society islands, basalt data do not seem in favor of substantial nitrogen subduction. The absence of an overwhelming recycling signature for nitrogen in MORB and most OIB has implications for the deep N cycle. The lack of recycled nitrogen may reflect a low slab/mantle nitrogen concentration ratio, as illustrated by the mass balance done in section 5.1.2: for MORB $\delta^{15}N$ to be accounted for, $[N]_{slabs}$ must be < $[N]_{mantle}$ by at least a factor of ~ 3.

The nitrogen behavior in subduction zones controls the slab/mantle N concentration ratio. In metamorphic rocks, nitrogen is hosted in the structures of minerals such as micas and illites, as NH_4^+ substituting for potassium (Bebout et al., 1992, Busigny et al., 2003; Nieder et al., 2011). Nitrogen is thought to be quantitatively retained within minerals during metamorphism, supporting efficient nitrogen recycling in the mantle (Bebout et al., 2013; Busigny et al., 2003). In modern subduction zones, slab-fluid temperatures are between 750 and 950 °C (Plank et al., 2009). However, the rocks studied in Busigny et al., (2003) and in Bebout et al., (2013) reached a peak temperature of ~630 °C (Busigny et al., 2003), well below temperatures relevant to slab devolatilization. Observations on metamorphic rocks are invaluable, but may only apply to fore-arc devolatilization and may not constrain sub-arc slab fluid losses.

Experimental evidence suggest that cold subduction zones would allow nitrogen to remain in slabs even past the region of sub-arc melting (Jackson et al., 2021; Mallik et al., 2018). In those slabs, recycled nitrogen would remain stable as NH_4^+ in potassium-bearing minerals throughout fluid losses (Watenphul et al., 2010, 2009). Under higher temperatures relevant to hot subduction zones, laboratory experiments show a reversal of the nitrogen

504 partition coefficient, such that slab-nitrogen would be quantitatively lost during
505 devolatilization and mineral breakdown (Jackson et al., 2021). Füri et al., (2021) and Labidi
506 et al., (2021) showed that the mantle wedges of two distinct subduction zones are enriched
507 in N by ~ 1 to 2 orders of magnitude relative to the average MORB mantle. In the case of the
508 Central American hot subduction zone, the N enrichment in the mantle wedge is indicative
509 of near-quantitative nitrogen losses from the slab (Labidi et al., 2021). Overall, new
510 experimental and observational studies provide evidence that nitrogen losses during
511 devolatilization are substantial. In warm subduction zones, devolatilization would be nearly
512 quantitative, effectively preventing substantial N transfer to the deep mantle.

513 The perspective of limited nitrogen recycling may seem puzzling, partly because the
514 recycling of other volatiles in basalt sources is observed. For example, the budget of xenon
515 in MORB and OIB sources is dominated by 80-90% of a surface-derived component,
516 independently of basalt enrichments (Parai et al., 2019; Parai and Mukhopadhyay, 2021).
517 This may reflect xenon concentrations to be far higher in slabs than in the rest of the mantle.
518 Thus, even minimal contributions of slabs, like in the sources of depleted MORB, would drive
519 the xenon budget to be dominated by surface-derived components. These circumstances are
520 unique to xenon. The krypton isotope signatures of high $^{3}He/^{4}He$ basalts from plumes
521 requires a substantially more limited regassed contribution than xenon (Péron et al., 2021).
522 The case for argon recycling is debated: mantle sources of high $^{3}He/^{4}He$ basalts have
523 $^{40}Ar/^{36}Ar$ of ~ 10,000 (Mukhopadhyay, 2012; Péron et al., 2016), which is lower than
524 $^{40}Ar/^{36}Ar$ estimates of the MORB mantle by at least a factor of 2. This may reflect the
525 signature of a less degassed mantle reservoir (Allègre et al., 1987) or evidence for ^{36}Ar
526 recycling in the sources of high $^{3}He/^{4}He$ basalts (Holland and Ballentine, 2006). A scenario

where ^{36}Ar recycling preferentially affects plume sources leaves unexplained the relatively high $^{3}He/^{36}Ar$ of plumes relative to MORB ($^{3}He/^{36}Ar$ data in Moreira et al., 1998, Mukhopadhyay, 2012, Peron et al., 2016). In contrast with ^{36}Ar subduction, neon recycling was suggested to affect the MORB mantle more than high $^{3}He/^{4}He$ plumes: OIB with the most primitive $^{3}He/^{4}He$ ratios show solar $^{20}Ne/^{22}Ne$ ratio (Williams and Mukhopadhyay, 2018). The recycling of surface-derived neon into the MORB mantle would have lowered its $^{20}Ne/^{22}Ne$ ratio by a limited but measurable amount, from ~ 13.4 to ~ 12.5 (Williams and Mukhopadhyay, 2018). Note that alternative hypotheses offer explanations for the MORB $^{20}Ne/^{22}Ne$ ratio without resorting to neon subduction (Moreira and Charnoz, 2016; Péron et al., 2016). The carbon budget also shows somewhat limited regassing signatures. The $CO_2/^{3}He$ ratios of depleted MORB is ~5.0×10^{8} (Marty and Zimmerman, 1999, Graham and Michael, 2021). Enriched MORB have higher $CO_2/^{3}He$, on average ~ 6.0×10^{9} (Graham and Michael, 2021, Marty and Zimmerman, 1999, Peron et al., 2019). The relationship between $CO_2/^{3}He$ and enrichment likely results from carbon recycling as an illustration of the marble-cake mantle (Marty and Zimmermann, 1999). The $CO_2/^{3}He$ ratio of Icelandic basalts is ~6.7×10^{8} (Colin et al., 2015), as low as values observed depleted MORB. The low $CO_2/^{3}He$ in Iceland was suggested to argue against carbon recycling in the high $^{3}He/^{4}He$ Iceland source (Colin et al., 2015). Other volatiles such as sulfur, water and halogens illustrate various degrees of recycling in mantle reservoirs (Bekaert et al., 2021). This brief literature survey shows that various volatiles show a spectrum of behaviors in subduction. This work suggests that nitrogen may not be tied to the species showing the highest recycling efficiencies.

5.4 What consequences for exchange scenarios?

Nitrogen subduction is not recorded in the composition of the convective mantle. This may appear to be in conflict with modern fluxes of nitrogen between Earth's reservoirs, seemingly requiring nitrogen subduction to be much higher than N_2 degassing (Busigny et al., 2011). Scenarios extrapolating modern fluxes to deep time predict the ancient atmosphere showed elevated N_2 concentration relative to modern air, possibly even accounting for the faint young sun paradox (Goldblatt et al., 2009). When articulated to specifically explain the N isotope imbalance between Earth's reservoirs, nitrogen regassing models posit that mantle and air $\delta^{15}N$ had an even larger nitrogen isotope disequilibrium in the past (Javoy, 1997). Secular evolutions for [N] and $\delta^{15}N$ are anticipated, but they have not been observed. The N_2 partial pressure of the atmosphere appears to not have substantially changed over geological time, or if anything, to have *increased* (Avice et al., 2018; Marty et al., 2013; Nishizawa et al., 2007; Som et al., 2016). The $\delta^{15}N$ of air appears to have remained broadly constant over time, as attested by $^{15}N/^{14}N$ ratios from hydrothermal fluid inclusions (Avice et al., 2018; Marty et al., 2013; Nishizawa et al., 2007). Ancient sediments are inconsistent with an isotope evolution of surface nitrogen outside of brief (but extreme) excursions (Ader et al., 2016; Stüeken et al., 2015; Thomazo et al., 2011). If anything, the $\delta^{15}N$ of ancient sediments has been recently suggested to be *negative* prior to metamorphism in one formation from Greenland (Stüeken et al., 2021), at odds with the requirements of *positive* $\delta^{15}N$ for old surface-derived N. On the mantle side, most diamonds with fibrous and peridotitic paragenesis also appear to reflect broadly invariant $\delta^{15}N$ of $\sim -4‰$ through geological times (Boyd and Pillinger, 1994; Cartigny et al., 2014, 1997; Javoy et al., 1984; Palot et al., 2012; Stachel et al., n.d.).

This leads to a conundrum: modern subduction fluxes require nitrogen exchange between two isotopically distinct reservoirs, but no observational record of that interaction is preserved. Fluxes of nitrogen subduction are by design derived from modern subduction zones (Busigny et al., 2011). In present day, subduction zones are dominated by relatively low temperature gradients compared to Proterozoic and Archean subduction zones (Martin and Moyen, 2002). However, most of Earth's history has been dominated by hot subduction zones (Antonelli et al., 2021; Keller and Schoene, 2018; Martin and Moyen, 2002). I speculate that extrapolating fluxes from warm subduction zones (rather than average modern subduction fluxes) would probably relieve the need for substantial N exchange between mantle and air, and essentially allow the N isotope imbalance to persist with time (Labidi et al., 2020). The corollary to this principle is that the N isotope disequilibrium between Earth's reservoir observed today would be a relatively ancient feature.

5.5 Why is plume nitrogen not isotopically solar?

In the $^{3}He/^{4}He$ mantle, solar $^{20}Ne/^{22}Ne$ ratios indicate that at least some of the Earth's parent bodies must have dissolved gases of the solar nebula (Williams and Mukhopadhyay, 2018). This would have occurred in a magma ocean stage, requiring that molten parent bodies were somehow put in contact with nebular gases. Because only a few high $^{3}He/^{4}He$ basalts show solar $^{20}Ne/^{22}Ne$ ratios (and not MORB), the plume mantle is the only reservoir sampled today that would have recorded interactions with solar gases. In this context, the absence of solar nitrogen with $\delta^{15}N \sim -387 \pm 8‰$ is noted as problematic (Barry and Hilton, 2016; Williams and Mukhopadhyay, 2018). Chondritic addition and/or subduction could

both be culprits for nitrogen-neon decoupling. In the latter case, recycled nitrogen would have replaced any solar components inherited from planetary formation (Barry and Hilton, 2016; Williams and Mukhopadhyay, 2018).

One can calculate how much solar N would be dissolved altogether with solar Ne. I estimate the highest amount of solar neon present in the OIB mantle using a $^{3}He/^{22}Ne$ of the plume mantle ~2 (Peron et al., 2016, Mukhopadhyay, 2012) and $^{20}Ne/^{22}Ne$ anywhere between 12.5 and 13.5 (Williams and Mukhopadhyay, 2018). I take the [^{3}He] concentration of the MORB source is 10^{-10} ccSTP/g ^{3}He (Moreira et al., 1998), and 10 times higher in the plume endmember, i.e. 10^{-9} ccSTP/g ^{3}He. This results in ~10^{-8} ccSTP/g Ne as the concentration of solar neon in Earth's plume mantle, or ~10^{-13} mol/g Ne. Knowing solar gas N/Ne ~ 1 (Anders and Grevesse, 1989; Lodders, 2003) and respective solubilities of gaseous species (Libourel et al., 2003 and references therein), the dissolution of ~10^{-13} mol/g of solar Ne would result in ~10^{-14} mol/g of solar N, or 0.007 ppt of solar N. This is 8 orders of magnitude lower than observables on Earth, and ~11 orders of magnitude lower than chondritic precursors making up the bulk Earth. Chondrites contain 400 to 3000 ppm N (Alexander et al., 2012; Pepin, 1991), so that solar gases are unlikely to impact the budget of N of any planetary reservoir made of any realistic parent body. This simple mass balance shows that subduction is not needed to explain the absence of solar nitrogen in deep mantle, if it may be genetically linked with any chondritic parent body.

5.6. Speculation about the origin of Earth's nitrogen

Some rare diamonds from Earth's mantle record extremely low $\delta^{15}N$, consistent with an EC parent bodies (Palot et al., 2012). One may then ask, why is the $\delta^{15}N$ of both MORB and OIB mantle both different from enstatite chondrite, if not because of subduction? Substantial future work is needed to determine what set of circumstances may allow the Earth's N isotope imbalance to have been set during planetary differentiation, once accretion was complete. Recent studies have investigated the nitrogen behavior during planetary formation, with a focus on the thermodynamics of accretion, differentiation, and magma ocean degassing (Bernadou et al., 2021; Boulliung et al., 2020; Grewal et al., 2021; Sossi et al., 2020). Evidently, the content of N in modern Earth's reservoirs could easily have been set by a competition between metal/silicate equilibria and magma ocean degassing. As pointed out by Boulliung et al., (2020), N^{3-} would substitute with O^{2-} ions, leading to the formations of X– N^{3-} complexes dominated by Si-N bonds (see also Libourel et al., 2003). Under this speciation, nitrogen becomes substantially more soluble than dissolved N_2 (Bernadou et al., 2021; Boulliung et al., 2020; Libourel et al., 2003). Isotopic fractionation is set by distinct average bonding strengths of an element between two phases. The obviously distinct bonding environments between N^{3-} in a silicate melt and gaseous N_2 may result in ^{15}N being preferentially partitioned in gaseous N_2. Depending on the magnitude of the isotopic fractionation, partial degassing of a magma ocean, once Earth's accretion was complete, could conceivably set the isotope difference between mantle and atmospheric N. This suggestion has recently received experimental interest (Dalou et al., 2022). The notion of magma ocean degassing causing ^{15}N depletions in residual nitrogen, in silicate melts with low fO_2, seems viable (Dalou et al., 2022). In this context, it is possible that the plume $\delta^{15}N$

642 values between air and MORB reflect the signature of mantle reservoir that underwent less
643 degassing during a magma ocean phase (and therefore less ^{15}N depletion) than the more
644 degassed convective mantle.

645 The $\delta^{15}N$ of Earth's mantle is higher than the enstatite chondrites average $\delta^{15}N$ of
646 $-20\pm11‰$ (1σ, Grady et al., 1986), at least at the 1σ level. This difference may have been set
647 by heterogeneous accretion. Carbonaceous chondrites could have contributed positive $\delta^{15}N$
648 to an EC-like Earth during either the main stages of accretion or via the addition of a late
649 veneer (Marty and Zimmermann, 1999; Piani et al., 2020). However, it is not clear whether
650 a substantial addition of carbonaceous chondrites, especially during late accretion, would
651 allow maintaining the EC-Earth similarity for a vast array of nucleosynthetic anomalies
652 (Dauphas, 2017).

653 Heterogeneous accretion may not be required to explain the $\delta^{15}N$ of Earth's mantle,
654 should planetary nitrogen undergo isotope fractionation(s) during Earth's formation and
655 differentiation. Metal/silicate fractionations could raise the mantle $\delta^{15}N$ from a starting
656 composition similar to EC, although there is debate as to what the true metal/silicate isotope
657 fractionation is for N (Dalou et al., 2019; Li et al., 2016). Isotope fractionation associated
658 with volatile losses described in Young et al., (2019) for other elements could also be
659 relevant. They are not mutually exclusive with metal/silicate fractionation, and their
660 combined effect on $\delta^{15}N$, $N_2/^3He$ and $N_2/^{36}Ar$ need to be investigated experimentally and
661 with first-principle calculations.

662

663

664

6. Conclusion

MORB and OIB nitrogen isotope data were compiled from the literature. After filtering out air-contaminated basalts, and correcting $N_2/^3He$ from fractional degassing, $\delta^{15}N$ and $N_2/^3He$ estimates can be obtained. MORB have $\delta^{15}N \sim 4‰$ and $N_2/^3He$ are $\sim 10^6$ on average. Both , $\delta^{15}N$ and $N_2/^3He$ appear invariant across vastly different degrees of mantle source enrichments. Notably, popping rocks have some of the highest K_2O/TiO_2 observed in MORB, but show $\delta^{15}N$ and $N_2/^3He$ indistinguishable from MORB. The invariant $\delta^{15}N$ and $N_2/^3He$ are fit with slabs containing ~0.1 ppm N at most. Slabs are required to show [N] ≤ 0.1 ppm N, mixed in a mantle with ~0.3 ppm N, for invariant $\delta^{15}N$ and $N_2/^3He$ at varying K_2O/TiO_2 to be accounted for. OIB are less well characterized than MORB for the nitrogen systematics. Extremely enriched mantle sources such as seen at the Society plume, where basalts show low $^3He/^4He$ ratios, are consistent with nitrogen subduction: erupted basalts have elevated $\delta^{15}N$ and $N_2/^3He$ ratios. On the other hand, OIB with high $^3He/^4He$ ratio have $\delta^{15}N$ between –2 and 0‰, and reconstructed $N_2/^3He$ that appear similar to MORB, across varying K_2O/TiO_2. This is not consistent with nitrogen subduction. Overall, published data argue against nitrogen recycling to overwhelm the modern mantle, for at least high $^3He/^4He$ OIB and MORB sources. Instead, mantle nitrogen with $\delta^{15}N \sim -4‰$ for MORB and between –2 and 0‰ for OIB, with $N_2/^3He \sim 10^6$, appear to be intrinsic features of Earth's interior, mostly disconnected from Earth's surface.

This conclusion has implications on the origin of Earth's N: $\delta^{15}N$ differences between the mantle and parent bodies similar to enstatite chondrites (or solar gases) may have to be explained without resorting to nitrogen subduction. It may reflect the contribution of carbonaceous chondrites to Earth's nitrogen budget. Alternatively, nitrogen isotope

688 fractionation during planetary formation may have been at play. Subsequent magma ocean
689 degassing under the restricted condition of low fO_2 could potentially yield the $\delta^{15}N$
690 disequilibrium between the MORB mantle and air. These two reservoirs would then remain
691 broadly unchanged, on account of a limited exchange via subduction. These hypotheses will
692 be largely testable with experimental and theoretical work.
693
694 **Acknowledgments**
695 JL thanks Pierre Cartigny, Guillaume Avice, James Dottin, Sandrine Péron, Thomas Giunta,
696 Colin Jackson and David Bekaert for notes and helpful discussions. Evelyn Füri, Sami Mikhail
697 and an anonymous reviewer are thanked for constructive and helpful reviews. Evelyn Füri
698 and Don Porcelli are thanked for an efficient editorial handling.
699
700 **Captions**

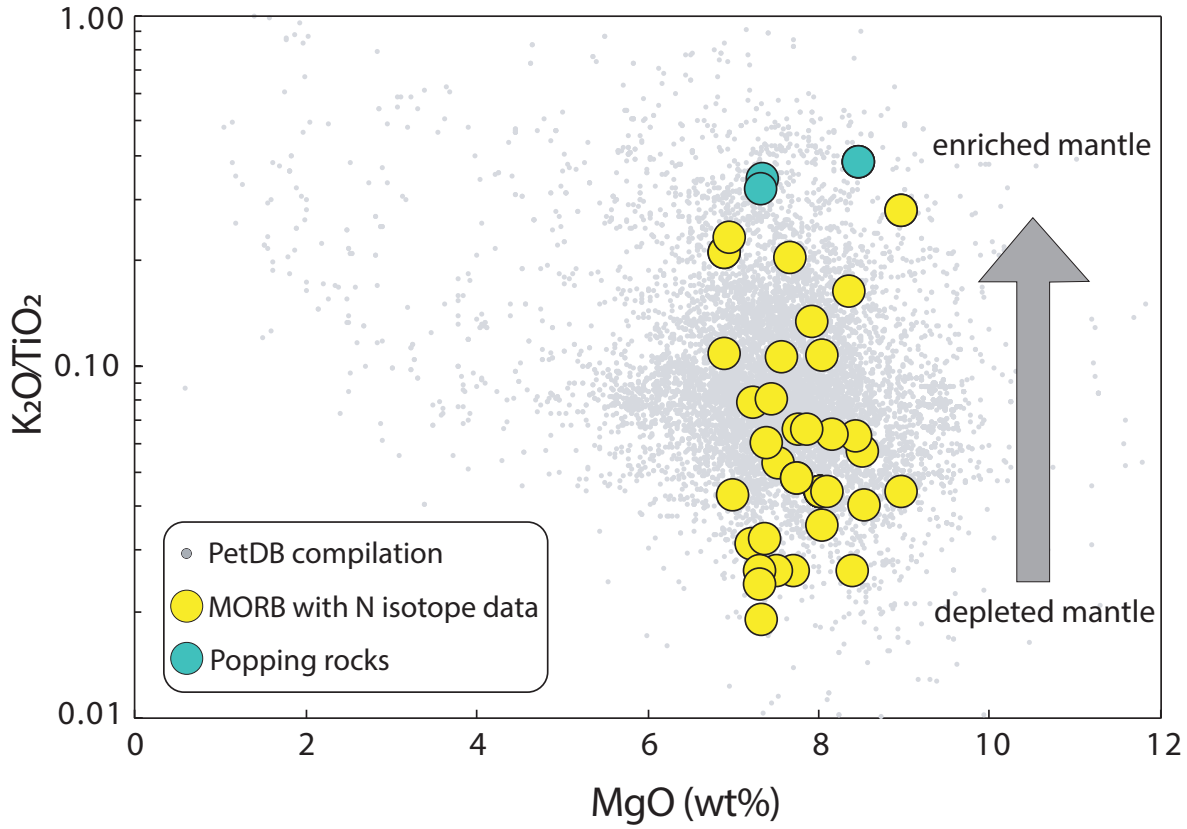

Figure 1

K_2O/TiO_2 ratios shown against magnesium oxide concentrations for mid-ocean ridge basalts. Worldwide MORB data are compiled using the PetDB database (Lehnert et al., 2000). Large symbols are for basalts with known N isotope composition. For popping rocks, data are combined from Javoy and Pineau (1991), Jones et al., (2019), Cartigny et al., (2008), Sarda and Graham (1989) and Labidi et al., (2020). For ordinary MORB, data are from Marty and Zimmermann (1999), Marty and Humbert (1997) and Barry and Hilton (2016). None of the basalts with published N isotope composition have MgO low enough to indicate titanomagnetite on the liquidus (MgO ≤ 4%), so their K_2O/TiO_2 are likely good tracers of the mantle source enrichments.

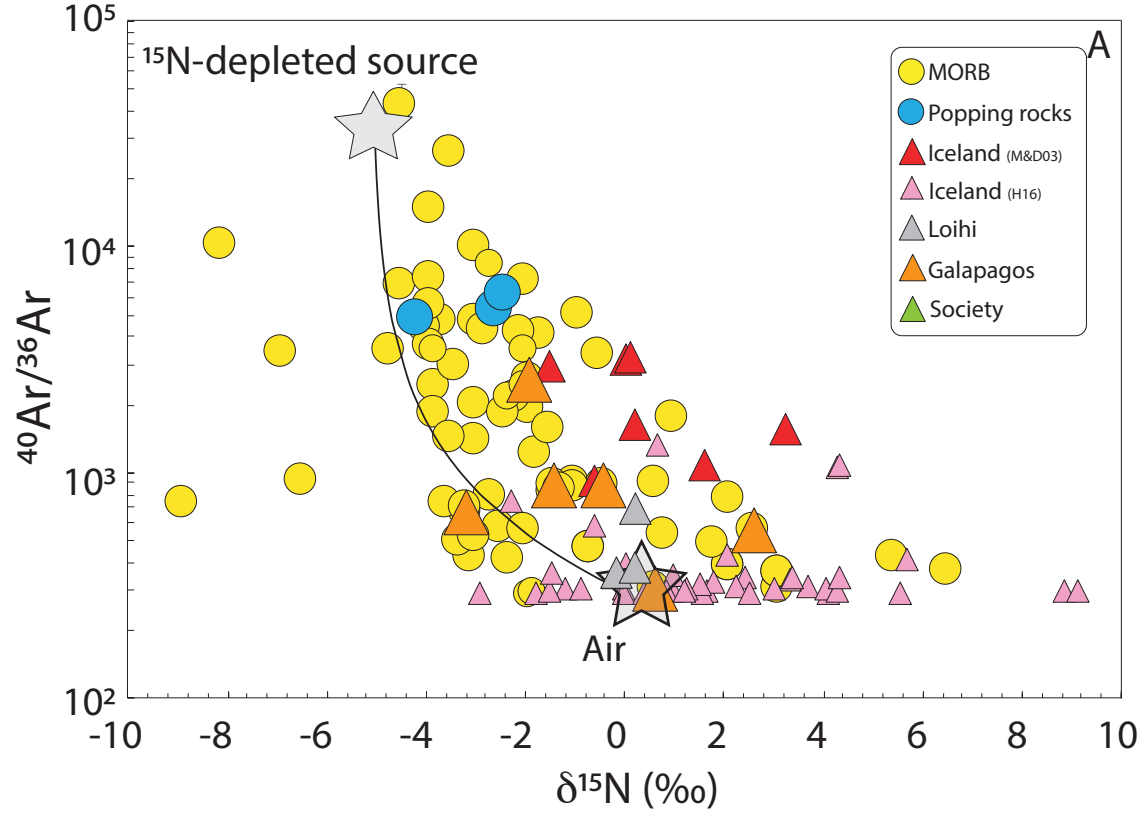
A
^{15}N-depleted source
MORB
Popping rocks
Iceland (M&D03)
Iceland (H16)
Loihi
Galapagos
Society
Air
^{40}Ar/^{36}Ar
δ^{15}N (‰)
10^5
10^4
10^3
10^2
-10
-8
-6
-4
-2
0
2
4
6
8
10

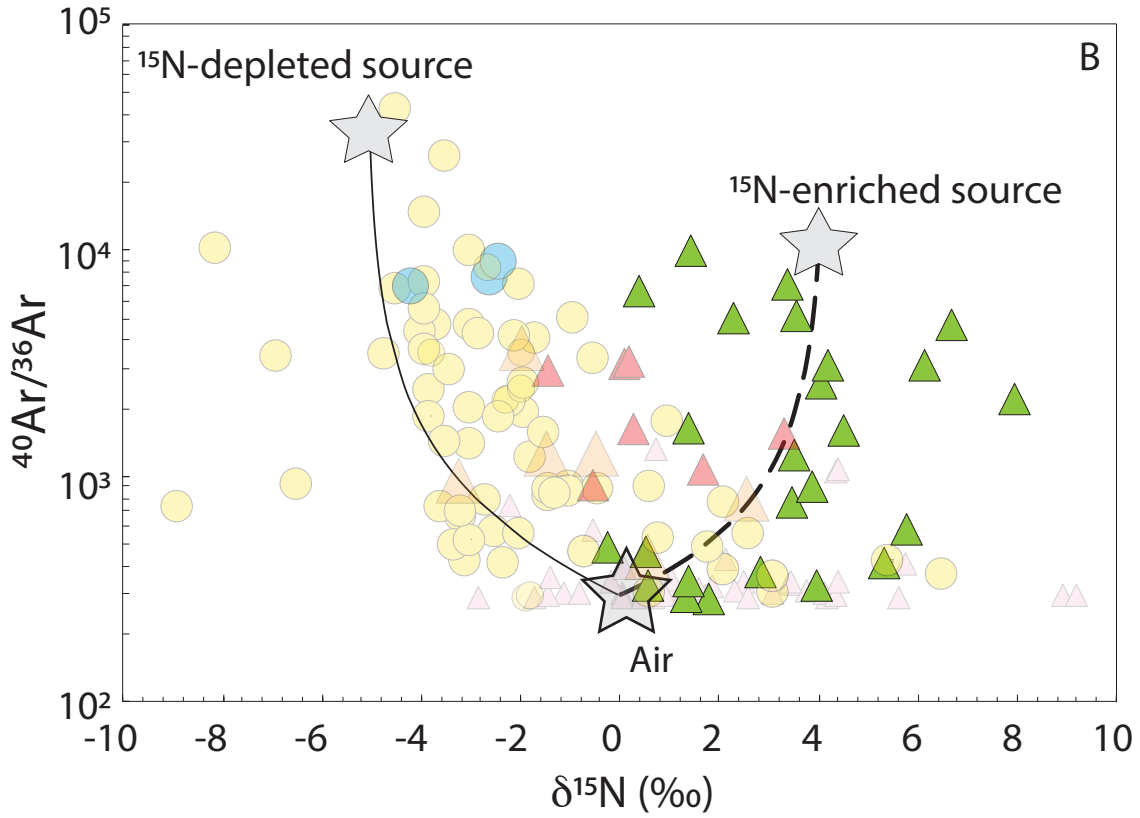
B
^{15}N-depleted source
^{15}N-enriched source
Air
^{40}Ar/^{36}Ar
δ^{15}N (‰)
10^5
10^4
10^3
10^2
-10
-8
-6
-4
-2
0
2
4
6
8
10

711

Figure 2

Published $\delta^{15}N$ data shown against $^{40}Ar/^{36}Ar$ ratios, for MORB and OIB. Data are compiled in Table 1 and 2, and are from the literature as discussed in the main text (Barry and Hilton, 2016; Halldórsson et al., 2016; Javoy and Pineau, 1991; Marty and Dauphas, 2003; Marty and Humbert, 1997; Marty and Zimmermann, 1999; Sano et al., 2001). On Panel A, worldwide MORB and high $^{3}He/^{4}He$ basalts from Hawaii, Galapagos and Iceland are shown. A mixing curve is drawn between air and the mantle. The curvature of the mixing relationship depends on the $N_2/^{36}Ar$ taken for air and mantle. A large majority of the samples are consistent with mantle endmembers (with $^{40}Ar/^{36}Ar > 5{,}000$) showing negative $\delta^{15}N$. MORB tend towards a $\delta^{15}N$ of ~–4‰. High $^{3}He/^{4}He$ OIB with the highest $^{40}Ar/^{36}Ar$ have $\delta^{15}N$ between –2 and 0‰. On Panel B, low $^{3}He/^{4}He$ lavas from Society are emphasized. They show distinctly high $\delta^{15}N$ at high $^{40}Ar/^{36}Ar$ ratios.

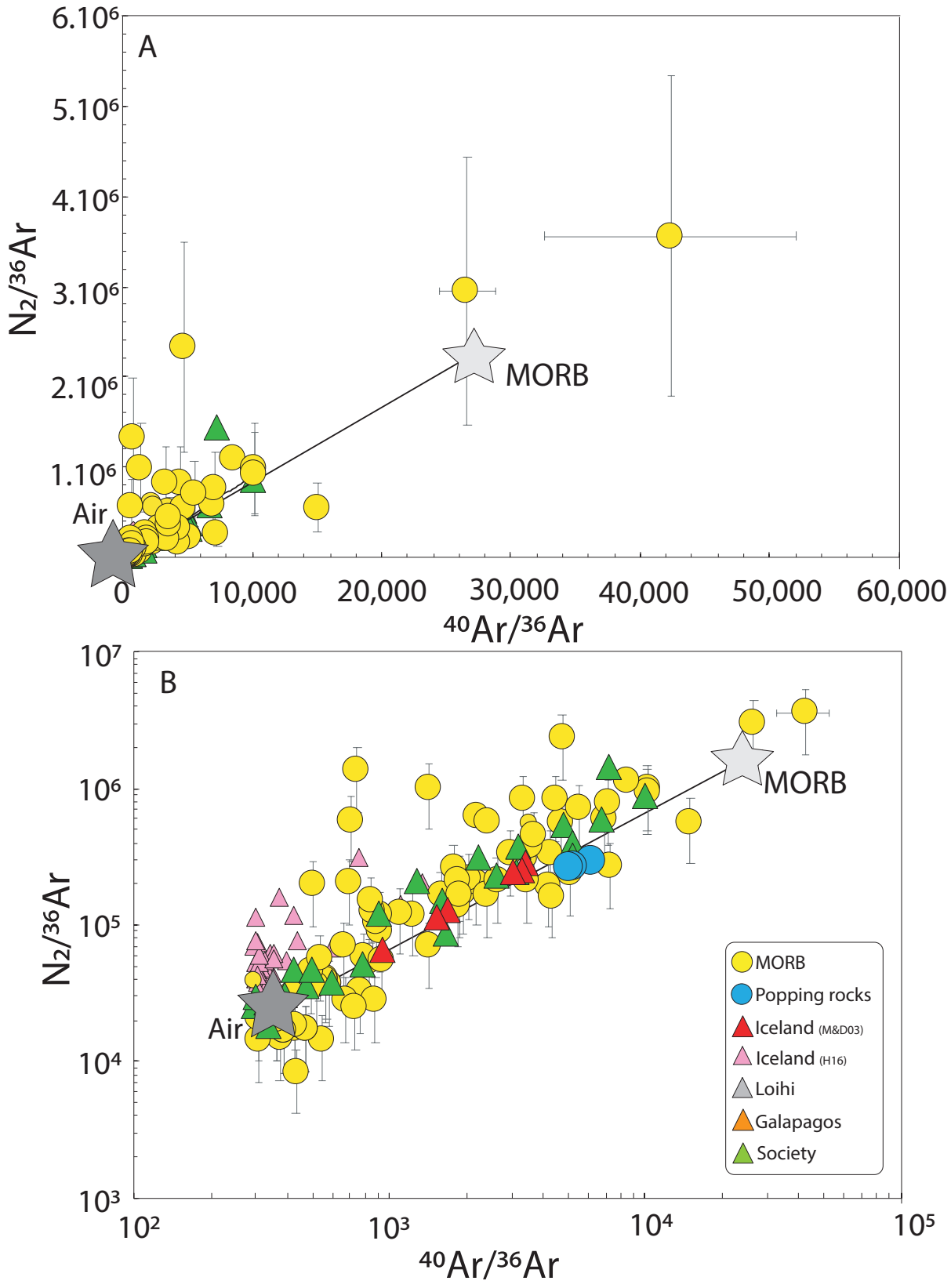
A
6.10⁶
5.10⁶
4.10⁶
3.10⁶
2.10⁶
1.10⁶
N2/36Ar
Air
MORB
0
10,000
20,000
30,000
40,000
50,000
60,000
40Ar/36Ar
B
10⁷
10⁶
10⁵
10⁴
10³
N2/36Ar
Air
MORB
10²
10³
10⁴
10⁵
40Ar/36Ar
MORB
Popping rocks
Iceland (M&D03)
Iceland (H16)
Loihi
Galapagos
Society

Figure 3

Basalts $N_2/^{36}Ar$ data plotted against $^{40}Ar/^{36}Ar$ ratios. The data source is the same as for figure 2. On panel A and B, the same dataset is shown using linear or using logarithm scales, respectively.

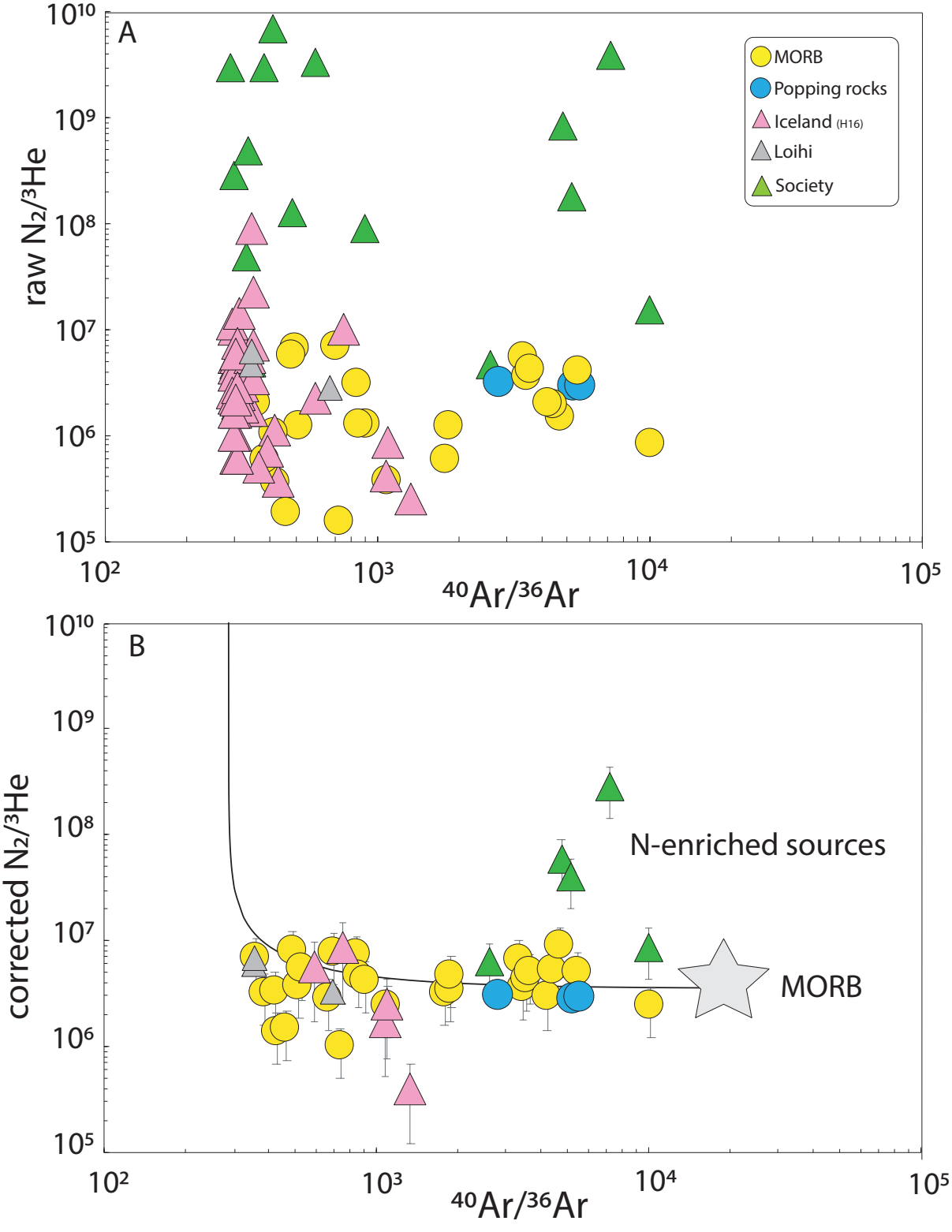

730
731 **Figure 4**

Basalts $N_2/^3He$ data shown against $^{40}Ar/^{36}Ar$ ratios. The data source is the same as for figure 2 and 3. On panel A, raw $N_2/^3He$ are plotted. On panel B, $N_2/^3He$ is corrected for fractional degassing (see text). Only samples with $^{40}Ar/^{36}Ar > 500$ are shown, thus avoiding the largely elevated $N_2/^3He$ ratios associated with air signatures, at $^{40}Ar/^{36}Ar < 500$.

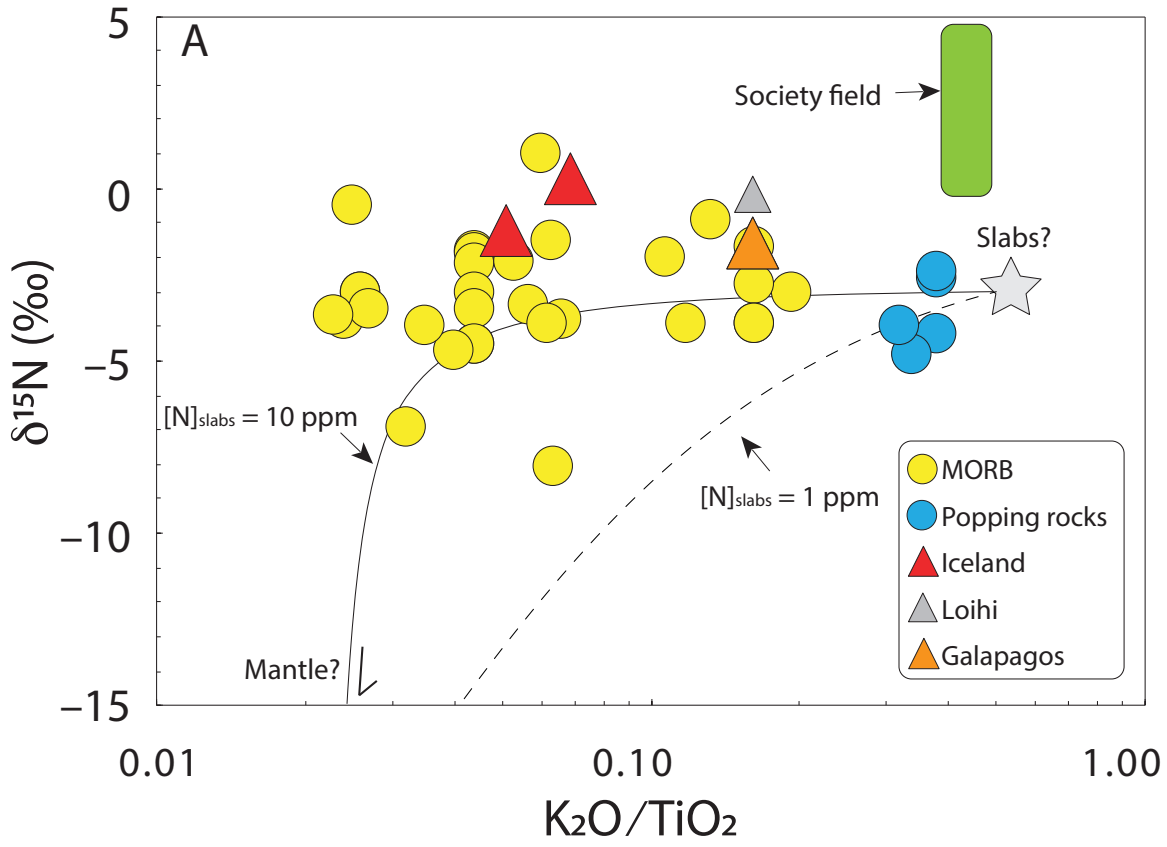
A
Society field
Slabs?
[N]slabs = 10 ppm
[N]slabs = 1 ppm
Mantle?
MORB
Popping rocks
Iceland
Loihi
Galapagos
δ15N (‰)
5
0
−5
−10
−15
0.01
0.10
1.00
K2O/TiO2

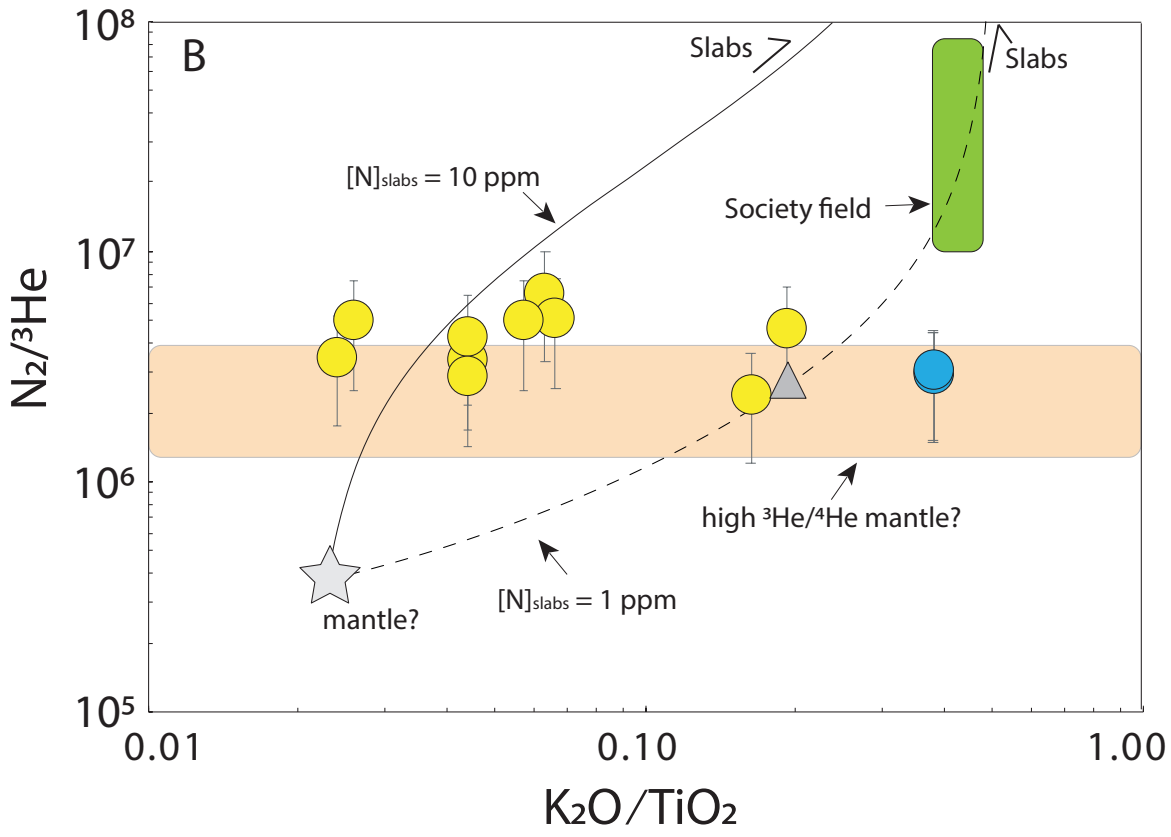
B
Slabs
Slabs
[N]slabs = 10 ppm
Society field
high 3He/4He mantle?
[N]slabs = 1 ppm
mantle?
N2/3He
10⁸
10⁷
10⁶
10⁵
0.01
0.10
1.00
K2O/TiO2

Figure 5

Nitrogen isotope data and $N_2/^3He$ ratios for MORB and OIB shown against K_2O/TiO_2 ratios. Only samples with high $^{40}Ar/^{36}Ar$ are used. A threshold of $^{40}Ar/^{36}Ar > 500$ was used. On panel A, 28 ordinary MORB, 3 popping rocks (including two duplicates of 2πD43) and 4 OIB pass the filter, and are plotted. On panel B, the same basalts are plotted, but only a fraction of them have published $N_2/^3He$ ratios. This results in only 10 ordinary MORB, 1 popping rock (three replicates of 2πD43) and one OIB to be plotted. The reconstructed $N_2/^3He$ field for OIB is shown (see text). For MORB, both $\delta^{15}N$ and $N_2/^3He$ ratios are invariant across a vast range of mantle enrichment. High $^3He/^4He$ OIB show a comparable data distribution, although it is much less well known. When $N_2/^3He$ ratios are not directly measured (e.g., DICE 10 and 11), or when K_2O/TiO_2 and $N_2/^3He$ ratios are not measured on the exact same basalts (e.g., Society samples), fields are shown for illustration. Mixing curves are shown, taking $[N]_{slabs}$ 1 and 10 ppm. Doing so allow a starting $\delta^{15}N$ of the mantle to be similar to enstatite chondrites as done here for illustration, but is allowed to be virtually be any value, including a CI–like or solar $\delta^{15}N$ of +48‰ and –387‰, respectively. This scenario requires improbable [N] and $\delta^{15}N$ signatures for recycled components, and fails at explaining the constant $N_2/^3He$ ratios of basalts across varying K_2O/TiO_2.

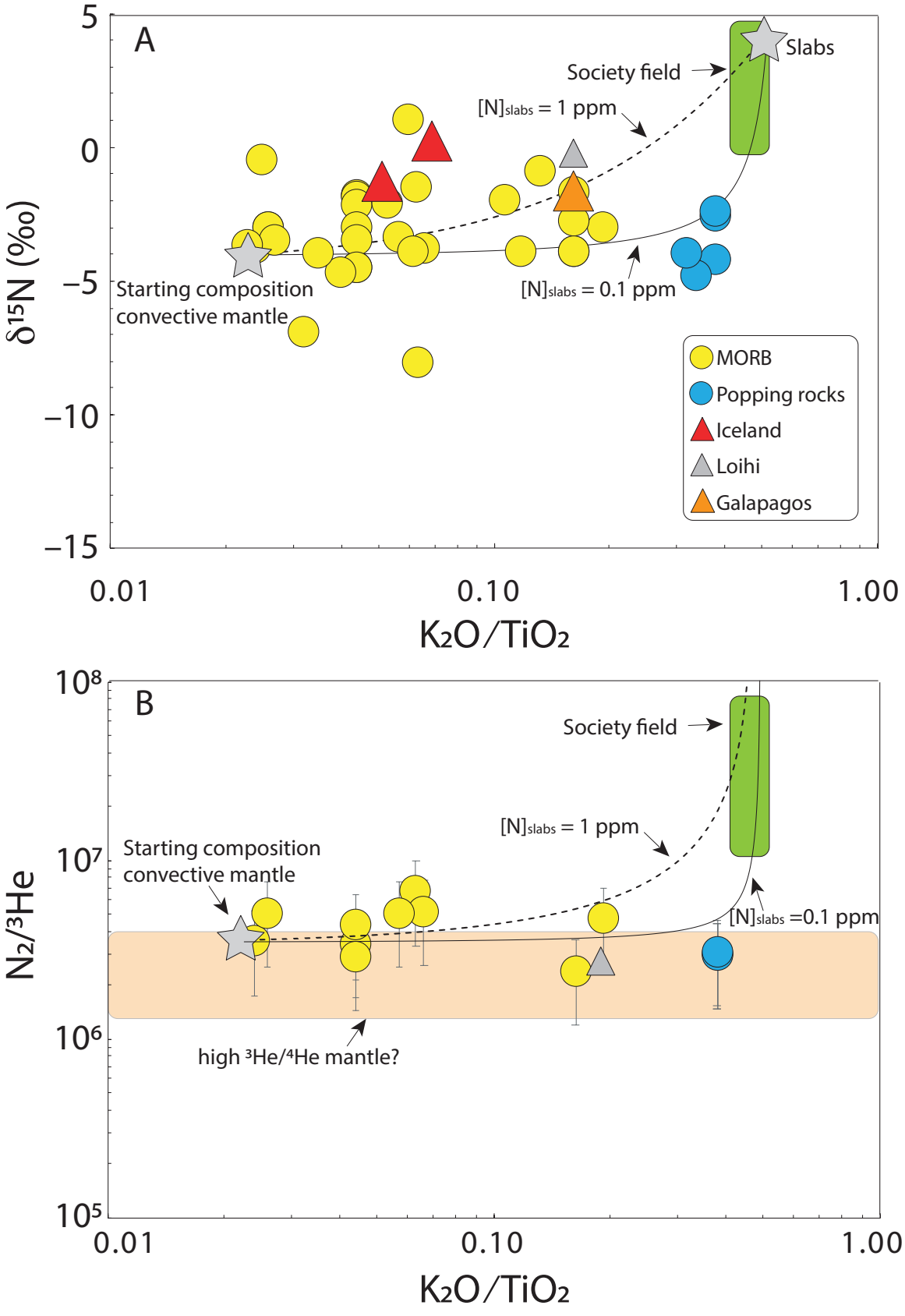
A
Slabs
Society field
[N]slabs = 1 ppm
[N]slabs = 0.1 ppm
Starting composition
convective mantle
MORB
Popping rocks
Iceland
Loihi
Galapagos
δ15N (‰)
5
0
−5
−10
−15
0.01
0.10
1.00
K2O/TiO2
B
Society field
[N]slabs = 1 ppm
Starting composition
convective mantle
[N]slabs =0.1 ppm
high 3He/4He mantle?
N2/3He
10^8
10^7
10^6
10^5
0.01
0.10
1.00
K2O/TiO2

Figure 6

Nitrogen isotope data and $N_2/^3He$ ratios for MORB and OIB shown against K_2O/TiO_2 ratios. Same data as in figure 5. Here, a set of mixing curve is shown, taking $[N]_{slabs} \sim 0.1$ ppm and 1 ppm N. Doing so require the starting $\delta^{15}N$ of the mantle to be similar to the modern value. The recycled components are taken with an elevated $\delta^{15}N$ (Busigny et al., 2011). Doing so results in flat relationships in both panels. The near-vertical part of the mixing hyperbolae happens to be consistent with the low $^3He/^4He$ Society basalts, that show elevated $\delta^{15}N$. This is at odds with OIB with high $^3He/^4He$. Their marginally high $\delta^{15}N$ and MORB like $N_2/^3He$ do not require nitrogen addition via subduction.

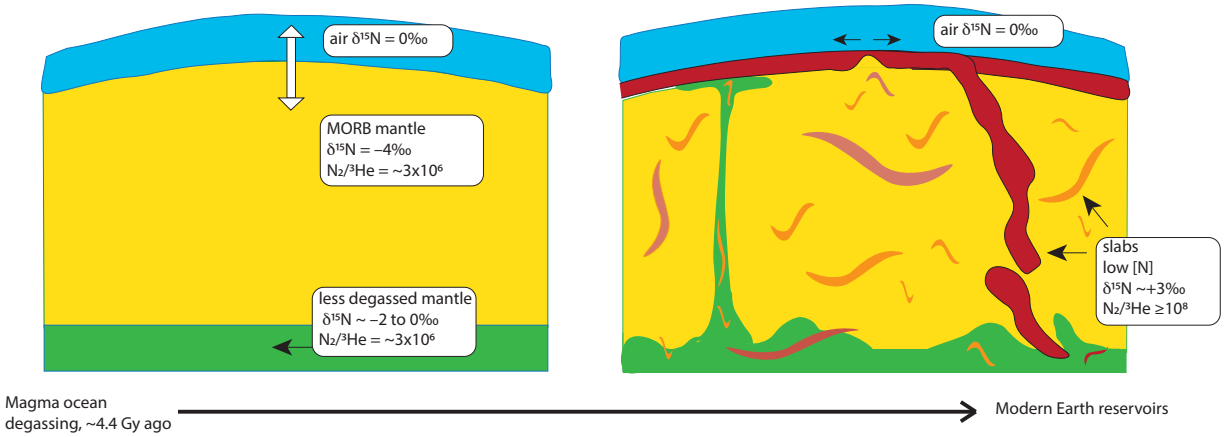

Figure 7

Cartoon showing the constraints on the origin of N in MORB and plume sources. The cartoon is largely inspired by the illustration in Parai et al., (2019), redrawn for the purpose of this work. Panels A, and B illustrate two snapshots in time. Panel A represents a tentative view of the solid mantle, immediately after the solidification of the magma ocean. Panel B represents modern day.

References

Abernethy, F.A.J., Verchovsky, A.B., Starkey, N.A., Anand, M., Franchi, I.A., Grady, M.M., 2013. Stable isotope analysis of carbon and nitrogen in angrites. Meteorit. Planet. Sci. n/a-n/a. https://doi.org/10.1111/maps.12184

Ader, M., Thomazo, C., Sansjofre, P., Busigny, V., Papineau, D., Laffont, R., Cartigny, P., Halverson, G.P., 2016. Interpretation of the nitrogen isotopic composition of Precambrian sedimentary rocks: Assumptions and perspectives. Chem. Geol. 429, 93–110.

Alexander, C.M.O., Bowden, R., Fogel, M.L., Howard, K.T., Herd, C.D.K., Nittler, L.R., 2012. The provenances of asteroids, and their contributions to the volatile inventories of the terrestrial planets. Science (80-.). 337, 721–723. https://doi.org/10.1126/science.1223474

Allègre, C.J., Staudacher, T., Sarda, P., 1987. Rare gas systematics: formation of the atmosphere, evolution and structure of the Earth's mantle. Earth Planet. Sci. Lett. 81, 127–150. https://doi.org/http://dx.doi.org/10.1016/0012-821X(87)90151-8

Allègre, C.J., Turcotte, D.L., 1986. Implications of a two-component marble-cake mantle. Nature 323, 123.

Anders, E., Grevesse, N., 1989. Abundances of the elements: Meteoritic and solar. Geochim. Cosmochim. Acta 53, 197–214.

Antonelli, M.A., Kendrick, J., Yakymchuk, C., Guitreau, M., Mittal, T., Moynier, F., 2021. Calcium isotope evidence for early Archaean carbonates and subduction of oceanic crust. Nat. Commun. 12, 1–8.

Avice, G., Marty, B., Burgess, R., Hofmann, A., Philippot, P., Zahnle, K., Zakharov, D., 2018. Evolution of atmospheric xenon and other noble gases inferred from Archean to Paleoproterozoic rocks. Geochim. Cosmochim. Acta 232, 82–100.

Bach, W., Hegner, E., Erzinger, J., Satir, M., 1994. Chemical and isotopic variations along the superfast spreading East Pacific Rise from 6 to 30 S. Contrib. to Mineral. Petrol. 116, 365–380.

Barry, P.H., Hilton, D.R., 2016. Release of subducted sedimentary nitrogen throughout Earth's mantle. Geochemical Perspect. Lett. 2, 148–159. https://doi.org/http://dx.doi.org/10.7185/geochemlet.1615

Bebout, G.E., Agard, P., Kobayashi, K., Moriguti, T., Nakamura, E., 2013. Devolatilization history and trace element mobility in deeply subducted sedimentary rocks: Evidence from Western Alps HP/UHP suites. Chem. Geol. 342, 1–20.

Bebout, G.E., Fogel, M.L., 1992. Nitrogen-isotope compositions of metasedimentary rocks in the Catalina Schist, California: implications for metamorphic devolatilization history. Geochim. Cosmochim. Acta 56, 2839–2849.

Bekaert, D.V., Turner, S.J., Broadley, M.W., Barnes, J.D., Halldórsson, S.A., Labidi, J., Wade, J., Walowski, K.J., Barry, P.H., 2021. Subduction-Driven Volatile Recycling: A Global Mass Balance. Annu. Rev. Earth Planet. Sci. 49.

Bernadou, F., Gaillard, F., Füri, E., Marrocchi, Y., Slodczyk, A., 2021. Nitrogen solubility in basaltic silicate melt-Implications for degassing processes. Chem. Geol. 573, 120192.

Boulliung, J., Füri, E., Dalou, C., Tissandier, L., Zimmermann, L., Marrocchi, Y., 2020. Oxygen fugacity and melt composition controls on nitrogen solubility in silicate melts. Geochim. Cosmochim. Acta 284, 120–133.

Boyd, S.R., Pillinger, C.T., 1994. A preliminary study of 15N14N in octahedral growth form diamonds. Chem. Geol. 116, 43–59.

Brandon, A.D., Graham, D.W., Waight, T., Gautason, B., 2007. 186Os and 187Os enrichments and high-3He/4He sources in the Earth's mantle: evidence from Icelandic picrites. Geochim. Cosmochim. Acta 71, 4570–4591.

Busigny, V., Cartigny, P., Laverne, C., Teagle, D., Bonifacie, M., Agrinier, P., 2019. A re-assessment of the nitrogen geochemical behavior in upper oceanic crust from Hole 504B: Implications for subduction budget in Central America. Earth Planet. Sci. Lett. 525, 115735.

Busigny, V., Cartigny, P., Philippot, P., 2011. Nitrogen isotopes in ophiolitic metagabbros: A re-evaluation of modern nitrogen fluxes in subduction zones and implication for the early Earth atmosphere. Geochim. Cosmochim. Acta 75, 7502–7521. https://doi.org/10.1016/j.gca.2011.09.049

Busigny, V., Cartigny, P., Philippot, P., Ader, M., Javoy, M., 2003. Massive recycling of nitrogen and other fluid-mobile elements (K, Rb, Cs, H) in a cold slab environment: evidence from HP to UHP oceanic metasediments of the Schistes Lustrés nappe (western Alps, Europe). Earth Planet. Sci. Lett. 215, 27–42. https://doi.org/10.1016/s0012-821x(03)00453-9

Cartigny, P., Boyd, S., Harris, J., Javoy, M., 1997. Nitrogen isotopes in peridotitic diamonds from Fuxian, China: the mantle signature. Terra Nov. 9, 175–179.

Cartigny, P., Jendrzejewski, N., Pineau, F., Petit, E., Javoy, M., 2001. Volatile (C, N, Ar) variability in MORB and the respective roles of mantle source heterogeneity and degassing: the case of the Southwest Indian Ridge. Earth Planet. Sci. Lett. 194, 241–257.

Cartigny, P., Marty, B., 2013. Nitrogen isotopes and mantle geodynamics: The emergence of life and the atmosphere–crust–mantle connection. Elements 9, 359–366.

Cartigny, P., Palot, M., Thomassot, E., Harris, J.W., 2014. Diamond Formation: A Stable Isotope Perspective. Annu. Rev. Earth Planet. Sci. 42, 699–732. https://doi.org/10.1146/annurev-earth-042711-105259

Cartigny, P., Pineau, F., Aubaud, C., Javoy, M., 2008. Towards a consistent mantle carbon flux estimate: Insights from volatile systematics (H2O/Ce, δD, CO2/Nb) in the North Atlantic mantle (14°N and 34°N). Earth Planet. Sci. Lett. 265, 672–685.

Chauvel, C., Hofmann, A.W., Vidal, P., 1992. HIMU-EM: the French Polynesian connection. Earth Planet. Sci. Lett. 110, 99–119.

Colin, A., Moreira, M., Gautheron, C., Burnard, P., 2015. Constraints on the noble gas composition of the deep mantle by bubble-by-bubble analysis of a volcanic glass sample from Iceland. Chem. Geol. 417, 173–183. https://doi.org/http://dx.doi.org/10.1016/j.chemgeo.2015.09.020

Dalou, C., Deligny, C., Füri, E., 2022. Nitrogen isotope fractionation during magma ocean degassing: tracing the composition of early Earth's atmosphere. Geochemical Perspect. Lett. 20, 27–31.

Dalou, C., Furi, E., Deligny, C., Piani, L., Caumon, M.C., Laumonier, M., Boulliung, J., Eden, M., 2019. Redox control on nitrogen isotope fractionation during planetary core formation. Proc Natl Acad Sci U S A 116, 14485–14494. https://doi.org/10.1073/pnas.1820719116

Dauphas, N., 2017. The isotopic nature of the Earth's accreting material through time. Nature 541, 521–524. https://doi.org/10.1038/nature20830

Dauphas, N., Marty, B., 1999. Heavy nitrogen in carbonatites of the Kola Peninsula: A possible signature of the deep mantle. Science (80-.). 286, 2488–2490.

Dosso, L., Bougault, H., Langmuir, C., Bollinger, C., Bonnier, O., Etoubleau, J., 1999. The age and distribution of mantle heterogeneity along the Mid-Atlantic Ridge (31–41 N). Earth Planet. Sci. Lett. 170, 269–286.

Farley, K.A., Natland, J.H., Craig, H., 1992. Binary mixing of enriched and undegassed (primitive?) mantle components (He, Sr, Nd, Pb) in Samoan lavas. Earth Planet. Sci. Lett. 111, 183–199.

Fischer, T.P., Hilton, D.R., Zimmer, M.M., Shaw, A.M., Sharp, Z.D., Walker, J.A., 2002. Subduction and recycling of nitrogen along the Central American margin. Science (80-.). 297, 1154–1157.

Füri, E., Hilton, D.R., Halldórsson, S.A., Barry, P.H., Hahm, D., Fischer, T.P., Grönvold, K., 2010. Apparent decoupling of the He and Ne isotope systematics of the Icelandic mantle: The role of He depletion, melt mixing, degassing fractionation and air interaction. Geochim. Cosmochim. Acta 74, 3307–3332. https://doi.org/10.1016/j.gca.2010.03.023

Füri, E., Marty, B., 2015. Nitrogen isotope variations in the Solar System. Nat. Geosci. 8, 515–522. https://doi.org/10.1038/ngeo2451

Füri, E., Portnyagin, M., Mironov, N., Deligny, C., Gurenko, A., Botcharnikov, R., Holtz, F., 2021. In situ quantification of the nitrogen content of olivine-hosted melt inclusions from Klyuchevskoy volcano (Kamchatka): Implications for nitrogen recycling at subduction zones. Chem. Geol. 120456.

Geist, D.J., Fornari, D.J., Kurz, M.D., Harpp, K.S., Adam Soule, S., Perfit, M.R., Koleszar, A.M., 2006. Submarine Fernandina: Magmatism at the leading edge of the Galápagos hot spot. Geochemistry, Geophys. Geosystems 7.

Goldblatt, C., Claire, M.W., Lenton, T.M., Matthews, A.J., Watson, A.J., Zahnle, K.J., 2009. Nitrogen-enhanced greenhouse warming on early Earth. Nat. Geosci. 2, 891–896.

Grady, M., Wright, I., 2003. Elemental and Isotopic Abundances of Carbon and Nitrogen in Meteorites. Space Sci. Rev. 106, 231–248. https://doi.org/10.1023/a:1024645906350

Graham, D.W., 2002. Noble gas isotope geochemistry of mid-ocean ridge and ocean island basalts: Characterization of mantle source reservoirs. Rev. Mineral. geochemistry 47, 247–317.

Grewal, D.S., Dasgupta, R., Hough, T., Farnell, A., 2021. Rates of protoplanetary accretion and differentiation set nitrogen budget of rocky planets. Nat. Geosci. 1–8.
Haendel, D., Mühle, K., Nitzsche, H.-M., Stiehl, G., Wand, U., 1986. Isotopic variations of the fixed nitrogen in metamorphic rocks. Geochim. Cosmochim. Acta 50, 749–758.
Halldórsson, S.A., Hilton, D.R., Barry, P.H., Füri, E., Grönvold, K., 2016. Recycling of crustal material by the Iceland mantle plume: New evidence from nitrogen elemental and isotope systematics of subglacial basalts. Geochim. Cosmochim. Acta 176, 206–226.
Halliday, A.N., 2013. The origins of volatiles in the terrestrial planets. Geochim. Cosmochim. Acta 105, 146–171. https://doi.org/http://dx.doi.org/10.1016/j.gca.2012.11.015
Hamelin, C., Dosso, L., Hanan, B.B., Moreira, M., Kositsky, A.P., Thomas, M.Y., 2011. Geochemical portray of the Pacific Ridge: New isotopic data and statistical techniques. Earth Planet. Sci. Lett. 302, 154–162.
Hémond, C., Devey, C.W., Chauvel, C., 1994. Source compositions and melting processes in the Society and Austral plumes (South Pacific Ocean): Element and isotope (Sr, Nd, Pb, Th) geochemistry. Chem. Geol. 115, 7–45.
Hilton, D.R., Fischer, T.P., Marty, B., 2002. Noble gases and volatile recycling at subduction zones. Rev. Mineral. geochemistry 47, 319–370.
Hilton, D.R., Grönvold, K., Macpherson, C.G., Castillo, P.R., 1999. Extreme 3He/4He ratios in northwest Iceland: constraining the common component in mantle plumes. Earth Planet. Sci. Lett. 173, 53–60.
Hirschmann, M.M., 2018. Comparative deep Earth volatile cycles: The case for C recycling from exosphere/mantle fractionation of major (H2O, C, N) volatiles and from H2O/Ce, CO2/Ba, and CO2/Nb exosphere ratios. Earth Planet. Sci. Lett. 502, 262–273.
Holland, G., Ballentine, C.J., 2006. Seawater subduction controls the heavy noble gas composition of the mantle. Nature 441, 186–191. https://doi.org/10.1038/nature04761
Jackson, C.R.M., Cottrell, E., Andrews, B., 2021. Warm and oxidizing slabs limit ingassing efficiency of nitrogen to the mantle. Earth Planet. Sci. Lett. 553, 116615.
Jackson, M.G., Blichert-Toft, J., Halldórsson, S.A., Mundl-Petermeier, A., Bizimis, M., Kurz, M.D., Price, A.A., Harðardóttir, S., Willhite, L.N., Breddam, K., 2020. Ancient helium and tungsten isotopic signatures preserved in mantle domains least modified by crustal recycling. Proc. Natl. Acad. Sci. 117, 30993–31001.
Jackson, M.G., Dasgupta, R., 2008. Compositions of HIMU, EM1, and EM2 from global trends between radiogenic isotopes and major elements in ocean island basalts. Earth Planet. Sci. Lett. 276, 175–186.
Javoy, M., 1998. The birth of the Earth's atmosphere: the behaviour and fate of its major elements. Chem. Geol. 147, 11–25.
Javoy, M., 1997. The major volatile elements of the Earth: Their origin, behavior, and fate. Geophys. Res. Lett. 24, 177–180.
Javoy, M., 1995. The integral enstatite chondrite model of the Earth. Geophys. Res. Lett. 22, 2219–2222.
Javoy, M., Pineau, F., 1991. The volatiles record of a "popping" rock from the Mid-Atlantic Ridge at 14°N: chemical and isotopic composition of gas trapped in the vesicles. Earth Planet. Sci. Lett. 107, 598–611.
Javoy, M., Pineau, F., Delorme, H., 1986. Carbon and nitrogen isotopes in the mantle. Chem. Geol. 57, 41–62.
Javoy, M., Pineau, F., Demaiffe, D., 1984. Nitrogen and carbon isotopic composition in the diamonds of Mbuji Mayi (Zaire). Earth Planet. Sci. Lett. 68, 399–412.
Jones, M.R., Wanless, V.D., Soule, S.A., Kurz, M.D., Mittelstaedt, E., Fornari, D.J., Curtice, J., Klein, F., Le Roux, V., Brodsky, H., 2019. New constraints on mantle carbon from Mid-Atlantic Ridge popping rocks. Earth Planet. Sci. Lett. 511, 67–75.
Keller, B., Schoene, B., 2018. Plate tectonics and continental basaltic geochemistry throughout Earth history. Earth Planet. Sci. Lett. 481, 290–304.
Kelley, K.A., Plank, T., Ludden, J., Staudigel, H., 2003. Composition of altered oceanic crust at ODP Sites 801 and 1149. Geochemistry, Geophys. Geosystems 4.
Kurz, M.D., Curtice, J., Fornari, D., Geist, D., Moreira, M., 2009. Primitive neon from the center of the Galápagos hotspot. Earth Planet. Sci. Lett. 286, 23–34.
Kurz, M.D., Jenkins, W.J., Hart, S.R., 1982. Helium isotopic systematics of oceanic islands and mantle heterogeneity. Nature 297, 43–47.
Labidi, J., Barry, P.H., Bekaert, D. V, Broadley, M.W., Marty, B., Giunta, T., Warr, O., Lollar, B.S., Fischer, T.P., Avice, G., 2020. Hydrothermal 15 N 15 N abundances constrain the origins of mantle nitrogen. Nature 580, 367–371.
Labidi, J., Young, E.D., 2022. The origin and dynamics of nitrogen in the Earth's mantle constrained by 15N15N in hydrothermal gases. Chem. Geol. 120709.
Labidi, J., Young, E.D., Fischer, T.P., Barry, P.H., Ballentine, C.J., de Moor, J.M., 2021. Recycling of nitrogen and light noble gases in the Central American subduction zone: constraints from 15N15N. Earth Planet. Sci. Lett.
Langmuir, C.H., Klein, E.M., Plank, T., 1992. Petrological systematics of mid-ocean ridge basalts: Constraints on melt generation beneath ocean ridges. Mantle flow melt Gener. mid-ocean ridges 71, 183–280.
Le Roex, A.P., Dick, H.J.B., Fisher, R.L., 1989. Petrology and geochemistry of MORB from 25 E to 46 E along the Southwest Indian Ridge: evidence for contrasting styles of mantle enrichment. J. Petrol. 30, 947–986.
Le Roux, P.J., Le Roex, A.P., Schilling, J.-G., Shimizu, N., Perkins, W.W., Pearce, N.J.G., 2002. Mantle heterogeneity beneath the southern Mid-Atlantic Ridge: trace element evidence for contamination of ambient asthenospheric mantle. Earth Planet. Sci. Lett. 203, 479–498.
Lehnert, K., Su, Y., Langmuir, C.H., Sarbas, B., Nohl, U., 2000. A global geochemical database structure for rocks. Geochemistry, Geophys. Geosystems 1.
Li, Y., Marty, B., Shcheka, S., Zimmermann, L., Keppler, H., 2016. Nitrogen isotope fractionation during terrestrial core-mantle separation. Geochemical Perspect. Lett. 2, 138–147. https://doi.org/http://dx.doi.org/10.7185/geochemlet.1614
Libourel, G., Marty, B., Humbert, F., 2003. Nitrogen solubility in basaltic melt. Part I. Effect of oxygen fugacity. Geochim. Cosmochim. Acta 67, 4123–4135. https://doi.org/10.1016/s0016-7037(03)00259-x
Lodders, K., 2003. Solar System abundances and condensation temperatures of the elements. Astrophys. J. 591, 1220–1247.
Mallik, A., Li, Y., Wiedenbeck, M., 2018. Nitrogen evolution within the Earth's atmosphere–mantle system assessed by recycling in subduction zones. Earth Planet. Sci. Lett. 482, 556–566.
Martin, H., Moyen, J.-F., 2002. Secular changes in tonalite-trondhjemite-granodiorite composition as markers of the progressive cooling of Earth. Geology 30, 319–322.

Marty, B., 2012. The origins and concentrations of water, carbon, nitrogen and noble gases on Earth. Earth Planet. Sci. Lett. 313–314, 56–66. https://doi.org/10.1016/j.epsl.2011.10.040
Marty, B., 1995. Nitrogen content of the mantle inferred from N2–Ar correlation in oceanic basalts. Nature 377, 326.
Marty, B., Almayrac, M., Barry, P.H., Bekaert, D. V, Broadley, M.W., Byrne, D.J., Ballentine, C.J., Caracausi, A., 2020. An evaluation of the C/N ratio of the mantle from natural CO2-rich gas analysis: geochemical and cosmochemical implications. Earth Planet. Sci. Lett. 551, 116574.
Marty, B., Avice, G., Sano, Y., Altwegg, K., Balsiger, H., Hässig, M., Morbidelli, A., Mousis, O., Rubin, M., 2016. Origins of volatile elements (H, C, N, noble gases) on Earth and Mars in light of recent results from the ROSETTA cometary mission. Earth Planet. Sci. Lett. 441, 91–102.
Marty, B., Dauphas, N., 2003. The nitrogen record of crust–mantle interaction and mantle convection from Archean to Present. Earth Planet. Sci. Lett. 206, 397–410. https://doi.org/10.1016/s0012-821x(02)01108-1
Marty, B., Humbert, F., 1997. Nitrogen and argon isotopes in oceanic basalts. Earth Planet. Sci. Lett. 152, 101–112.
Marty, B., Zimmermann, L., 1999. Volatiles (He, C, N, Ar) in mid-ocean ridge basalts: Assesment of shallow-level fractionation and characterization of source composition. Geochim. Cosmochim. Acta 63, 3619–3633.
Marty, B., Zimmermann, L., Pujol, M., Burgess, R., Philippot, P., 2013. Nitrogen Isotopic Composition and Density of the Archean Atmosphere. Science (80-.). 342, 101–104. https://doi.org/10.1126/science.1240971
Michael, P.J., Cornell, W.C., 1998. Influence of spreading rate and magma supply on crystallization and assimilation beneath mid-ocean ridges: Evidence from chlorine and major element chemistry of mid-ocean ridge basalts. J. Geophys. Res. Solid Earth 103, 18325–18356.
Moreira, M., 2013. Noble gas constraints on the origin and evolution of Earth's volatiles. Geochemical Perspect. 2, 229–230.
Moreira, M., Charnoz, S., 2016. The origin of the neon isotopes in chondrites and on Earth. Earth Planet. Sci. Lett. 433, 249–256. https://doi.org/http://dx.doi.org/10.1016/j.epsl.2015.11.002B
Moreira, M., Kunz, J., Allegre, C., 1998. Rare gas systematics in popping rock: isotopic and elemental compositions in the upper mantle. Science (80-.). 279, 1178–1181.
Mukhopadhyay, S., 2012. Early differentiation and volatile accretion recorded in deep-mantle neon and xenon. Nature 486, 101–104. https://doi.org/10.1038/nature11141
Mukhopadhyay, S., Parai, R., 2019. Noble gases: a record of Earth's evolution and mantle dynamics. Annu. Rev. Earth Planet. Sci. 47, 389–419.
Nishio, Y., Nakai, S., Ishii, T., Sano, Y., 2007. Isotope systematics of Li, Sr, Nd, and volatiles in Indian Ocean MORBs of the Rodrigues Triple Junction: Constraints on the origin of the DUPAL anomaly. Geochim. Cosmochim. Acta 71, 745–759.
Nishizawa, M., Sano, Y., Ueno, Y., Maruyama, S., 2007. Speciation and isotope ratios of nitrogen in fluid inclusions from seafloor hydrothermal deposits at~ 3.5 Ga. Earth Planet. Sci. Lett. 254, 332–344.
Palot, M., Cartigny, P., Harris, J.W., Kaminsky, F. V, Stachel, T., 2012. Evidence for deep mantle convection and primordial heterogeneity from nitrogen and carbon stable isotopes in diamond. Earth Planet. Sci. Lett. 357–358, 179–193. https://doi.org/http://dx.doi.org/10.1016/j.epsl.2012.09.015
Parai, R., Mukhopadhyay, S., 2021. Heavy noble gas signatures of the North Atlantic Popping Rock 2ПД43: Implications for mantle noble gas heterogeneity. Geochim. Cosmochim. Acta 294, 89–105.
Parai, R., Mukhopadhyay, S., Tucker, J.M., Pető, M.K., 2019. The emerging portrait of an ancient, heterogeneous and continuously evolving mantle plume source. Lithos 346, 105153.
Pearson, V.K., Sephton, M.A., Franchi, I.A., Gibson, J.M., Gilmour, I., 2006. Carbon and nitrogen in carbonaceous chondrites: Elemental abundances and stable isotopic compositions. Meteorit. Planet. Sci. 41, 1899–1918.
Pepin, R.O., 1991. On the origin and early evolution of terrestrial planet atmospheres and meteoritic volatiles. Icarus 92, 2–79.
Péron, S., Moreira, M., Colin, A., Arbaret, L., Putlitz, B., Kurz, M.D., 2016. Neon isotopic composition of the mantle constrained by single vesicle analyses. Earth Planet. Sci. Lett. 449, 145–154. https://doi.org/http://dx.doi.org/10.1016/j.epsl.2016.05.052
Péron, S., Moreira, M.A., Kurz, M.D., Curtice, J., Blusztajn, J.S., Putlitz, B., Wanless, V.D., Jones, M.R., Soule, S.A., Mittelstaedt, E., 2019. Noble gas systematics in new popping rocks from the Mid-Atlantic Ridge (14° N): Evidence for small-scale upper mantle heterogeneities. Earth Planet. Sci. Lett. 519, 70–82.
Péron, S., Mukhopadhyay, S., Kurz, M.D., Graham, D.W., 2021. Deep-mantle krypton reveals Earth's early accretion of carbonaceous matter. Nature 600, 462–467.
Piani, L., Marrocchi, Y., Rigaudier, T., Vacher, L.G., Thomassin, D., Marty, B., 2020. Earth's water may have been inherited from material similar to enstatite chondrite meteorites. Science (80-.). 369, 1110–1113.
Pinti, D.L., Hashizume, K., Matsuda, J., 2001. Nitrogen and argon signatures in 3.8 to 2.8 Ga metasediments: Clues on the chemical state of the Archean ocean and the deep biosphere. Geochim. Cosmochim. Acta 65, 2301–2315.
Plank, T., Cooper, L.B., Manning, C.E., 2009. Emerging geothermometers for estimating slab surface temperatures. Nat. Geosci. 2, 611–615.
Plank, T., Langmuir, C.H., 1998. The chemical composition of subducting sediment and its consequences for the crust and mantle. Chem. Geol. 145, 325–394.
Porcelli, D., Ballentine, C.J., Wieler, R., 2002. An Overview of Noble Gas Geochemistry and Cosmochemistry. Rev. Mineral. geochemistry 47, 1–19. https://doi.org/10.2138/rmg.2002.47.1
Raquin, A., Moreira, M.A., Guillon, F., 2008. He, Ne and Ar systematics in single vesicles: mantle isotopic ratios and origin of the air component in basaltic glasses. Earth Planet. Sci. Lett. 274, 142–150.
Reynolds, J.R., Langmuir, C.H., Bender, J.F., Kastens, K.A., Ryan, W.B.F., 1992. Spatial and temporal variability in the geochemistry of basalts from the East Pacific Rise. Nature 359, 493–499.
Sano, Y., Takahata, N., Nishio, Y., Fischer, T.P., Williams, S.N., 2001. Volcanic flux of nitrogen from the Earth. Chem. Geol. 171, 263–271.
Sarda, P., Graham, D., 1990. Mid-ocean ridge popping rocks: implications for degassing at ridge crests. Earth Planet. Sci. Lett. 97, 268–289.
Sarda, P., Staudacher, T., Allègre, C.J., 1988. Neon isotopes in submarine basalts. Earth Planet. Sci. Lett. 91, 73–88.
Schilling, J.G., Zajac, M., Evans, R., Johnston, T., White, W., Devine, J.D., Kingsley, R., 1983. Petrologic and geochemical variations along the Mid-Atlantic Ridge from 29 degrees N to 73 degrees N. Am. J. Sci. 283, 510–586.
Shen, Y., Forsyth, D.W., 1995. Geochemical constraints on initial and final depths of melting beneath mid-ocean ridges. J. Geophys. Res. Solid Earth 100, 2211–2237.

Smye, A.J., Jackson, C.R.M., Konrad-Schmolke, M., Hesse, M.A., Parman, S.W., Shuster, D.L., Ballentine, C.J., 2017. Noble gases recycled into the mantle through cold subduction zones. Earth Planet. Sci. Lett. 471, 65–73. https://doi.org/10.1016/j.epsl.2017.04.046

Sobolev, A. V, Hofmann, A.W., Kuzmin, D. V, Yaxley, G.M., Arndt, N.T., Chung, S.-L., Danyushevsky, L. V, Elliott, T., Frey, F.A., Garcia, M.O., 2007. The amount of recycled crust in sources of mantle-derived melts. Science (80-.). 316, 412–417.

Som, S.M., Buick, R., Hagadorn, J.W., Blake, T.S., Perreault, J.M., Harnmeijer, J.P., Catling, D.C., 2016. Earth's air pressure 2.7 billion years ago constrained to less than half of modern levels. Nat. Geosci. 9, 448–451.

Sossi, P.A., Burnham, A.D., Badro, J., Lanzirotti, A., Newville, M., O'Neill, H.S.C., 2020. Redox state of Earth's magma ocean and its Venus-like early atmosphere. Sci. Adv. 6, eabd1387.

Stachel, T., Cartigny, P., Chacko, T., Pearson, D.G., n.d. Carbon and Nitrogen in Mantle-Derived Diamonds. Rev. Mineral. geochemistry. https://doi.org/http://dx.doi.org/10.2138/rmg.2020.86.X

Staudacher, T., Allègre, C.J., 1988. Recycling of oceanic crust and sediments: the noble gas subduction barrier. Earth Planet. Sci. Lett. 89, 173–183.

Staudacher, T., Sarda, P., Richardson, S.H., Allègre, C.J., Sagna, I., Dmitriev, L. V, 1989. Noble gases in basalt glasses from a Mid-Atlantic Ridge topographic high at 14 N: geodynamic consequences. Earth Planet. Sci. Lett. 96, 119–133.

Stüeken, E.E., Boocock, T., Szilas, K., Mikhail, S., Gardiner, N.J., 2021. Reconstructing nitrogen sources to Earth's earliest biosphere at 3.7 Ga. Front. Earth Sci.

Stüeken, E.E., Buick, R., Guy, B.M., Koehler, M.C., 2015. Isotopic evidence for biological nitrogen fixation by molybdenum-nitrogenase from 3.2 Gyr. Nature 520, 666–669.

Thomazo, C., Ader, M., Philippot, P., 2011. Extreme 15N-enrichments in 2.72-Gyr-old sediments: evidence for a turning point in the nitrogen cycle. Geobiology 9, 107–120.

Trieloff, M., Kunz, J., Clague, D.A., Harrison, D., Allègre, C.J., 2000. The nature of pristine noble gases in mantle plumes. Science (80-.). 288, 1036–1038.

Watenphul, A., Wunder, B., Heinrich, W., 2009. High-pressure ammonium-bearing silicates: Implications for nitrogen and hydrogen storage in the Earth's mantle. Am. Mineral. 94, 283–292.

Watenphul, A., Wunder, B., Wirth, R., Heinrich, W., 2010. Ammonium-bearing clinopyroxene: a potential nitrogen reservoir in the Earth's mantle. Chem. Geol. 270, 240–248.

Williams, C.D., Mukhopadhyay, S., 2018. Capture of nebular gases during Earth's accretion is preserved in deep-mantle neon. Nature 565, 78–81. https://doi.org/10.1038/s41586-018-0771-1

Workman, R.K., Hart, S.R., 2005. Major and trace element composition of the depleted MORB mantle (DMM). Earth Planet. Sci. Lett. 231, 53–72.

Zimmer, M.M., Fischer, T.P., Hilton, D.R., Alvarado, G.E., Sharp, Z.D., Walker, J.A., 2004. Nitrogen systematics and gas fluxes of subduction zones: insights from Costa Rica arc volatiles. Geochemistry, Geophys. Geosystems 5.

Zindler, A., Hart, S., 1986. Chemical geodynamics. Annu. Rev. Earth Planet. Sci. 14, 493–571.